A QUANTITATIVE STUDY

INTO CARBON-IN-PULP

ADSORPTION OPERATIONS

BY

DIANE ELIZABETH GRAY

A THESIS SUBMITTED IN FULFILMENT OF THE REQUIREMENTS FOR
THE MASTERS DEGREE IN TECHNOLOGY
(CHEMICAL ENGINEERING)
AT THE CAPE TECHNIKON

SUPERVISOR: J.W. COETZEE

CAPE TECHNIKON
APRIL 1999

DECLARATION

I hereby certify that this thesis is my own original work, except where specifically acknowledged in the text.

.....

D.E. Gray
15 April 1999

ABSTRACT

Carbon-in-pulp (CIP) and carbon-in-leach (CIL) remain the most effective, and widely used processes for gold recovery from cyanided pulps. The extensive use of carbon in such processes have prompted many researchers to investigate the mechanism of metal cyanide adsorption. Not only has this provided many viable theories in the understanding of the mechanism, but it has also led to an improved understanding of the effects of the various operating conditions on the CIP circuit. However, the declining gold price has made gold producers aware of the need to either further optimise existing circuits or find alternative means of operation so as to improve efficiency. It is therefore the aim of this study to investigate the factors which influence the metal extraction circuit.

In this study the effects of parameters such as gold and carbon concentrations, slurry density and stirring speed on the adsorption process were investigated. It was found that the effects of gold and carbon concentrations could be determined directly, that is, a definite linear relationship exists between these two parameters and adsorption rate. However, slurry density and stirring speed (power input) have a twofold effect on the process. For this reason two distinct terms called the "blinding" and "mixing" numbers have been identified. It has been shown that all the parameters investigated influences the rate of adsorption during the constant rate adsorption period. However, only solution concentration, carbon concentration and carbon loading influence the process during the diminishing rate of adsorption. This confirmed the

belief that intraparticle diffusion is the rate controlling factor during the diminishing rate period. Furthermore, the point at which constant rate adsorption is replaced by the diminishing rate of adsorption is mainly a function of solution concentration.

ACKNOWLEDGEMENTS

The work contained in this thesis was carried out at the School of Mechanical and Process Engineering, Department of Chemical Engineering, at the Cape Technikon between January 1997 and December 1998.

I wish to thank the following people/institutions for their assistance and contributions in the completion of this thesis:

- The Department of Chemical Engineering at the Cape Technikon for the use of their instrumentation and laboratory facilities.
- The Foundation of Research Development (FRD) for their financial contribution to my work.
- My supervisor, Willie Coetzee, "thank you that your door was always open for all my problems and questions. I appreciate everything that you have done for me and all the time you put into helping me."
- To the staff and fellow students at the Cape Technikon, for all your help. To my friends, thank you for providing all the encouragement and laughter.
- My family, with your support and belief in me I know I can accomplish anything.
- Yuri, my fiancee, your love and encouragement has been amazing. Thank you for being so patient through all my years of studying.

CONTENTS

	PAGES
ABSTRACT	**i**
ACKNOWLEDGEMENTS	**iii**
CONTENTS	**iv**
LIST OF FIGURES	**viii**
LIST OF TABLES	**ix**
1. INTRODUCTION AND LITERATURE STUDY	**1**
1.1 ACTIVATED CARBON	1
1.1.1 Raw Materials	1
1.1.2 Physical Manufacture	2
1.1.2.1 Carbonisation	2
1.1.2.2 Activation	2
1.1.3 Chemical Manufacture	3
1.1.4 Physical Structure of Activated Carbon	3
1.1.5 Chemical Properties of Activated Carbon	5
1.2 GOLD BEARING ORES	5
1.2.1 Free milling ores	6
1.2.2 Refractory ores	6
1.3 CARBON-IN-PULP CIRCUIT	7
1.3.1 Adsorption	7
1.3.1.1 Tank size and layout	8
1.3.1.2 Mixing	8
1.3.1.3 Interstage screening	9
1.3.1.4 Carbon transfer	9
1.3.2 Elution	10
1.3.3 Carbon regeneration	10
1.3.4 Electrowinning	11
1.4 MECHANISMS FOR GOLD CYANIDE ADSORPTION	12

1.5 FACTORS AFFECTING GOLD CYANIDE ADSORPTION 12
1.5.1 Cyanide Concentration 12
1.5.2 Gold and Carbon Concentration 13
1.5.3 pH 13
1.5.4 Temperature 14
1.5.5 Free Ions (Ionic Strength) 14
1.5.6 Particle Size 15
1.5.7 Pulp Density 15

1.6 NON-IDEAL CONDITIONS 16
1.6.1 Back-mixing 16
1.6.2 Gold lock-up 17
1.6.3 Carbon breakage 17
1.6.4 Competitive adsorption with other species 18
1.6.5 Circuit foulants 18
1.6.6 Wood chips 19
1.6.7 Pregrobbing 20
1.6.8 Non-ideal mixing and retention time 20

1.7 ADSORPTION MODELING 20

1.8 LINEAR REGRESSION METHODS 22
1.8.1 Linear regression terms 22
1.8.2 Matrix approach to linear regression 22
1.8.3 Irregularities in linear regression 24
1.8.3.1 Hetroscedasticity 24
1.8.3.2 Multicollinearity 24
1.8.3.3 Autocorrellation 24

1.9 OBJECTIVES 24

2. THEORY 32

2.1 EQUILIBRIUM EXPRESSIONS 32
2.1.1 Linear isotherm 32
2.1.2 Freundlich isotherm 33
2.1.3 Langmuir isotherm 33

2.2 DIFFUSION MODEL: ASSUMPTIONS 33

2.3 MATERIAL BALANCE EQUATIONS 34

	2.4	PARAMETER ESTIMATION	36
	2.4.1	External mass transfer coefficient	36
	2.4.2	Intraparticle diffusivity	37
3.	**EXPERIMENTAL**		**38**
	3.1	EXPERIMENTAL MATERIAL	38
	3.2	EXPERIMENTAL SET-UP	39
	3.3	MINIMUM STIRRING SPEED	39
	3.4	EQUILIBRIUM ISOTHERM	40
	3.5	BATCH EXPERIMENTS	40
	3.6	ANALYTICAL METHODS	40
4.	**EQUILIBRIUM ISOTHERM**		**42**
	4.1	EQUILIBRIUM EXPERIMENTS	42
5.	**THE EFFECT OF DENSITY AND STIRRING SPEED ON THE EXTERNAL MASS TRANSFER COEFFICIENT**		**48**
	5.1	THE EFFECT OF SLURRY DENSITY	49
	5.2	THE EFFECT OF STIRRING SPEED	49
	5.3	THE EFFECTS OF GOLD AND CARBON CONCENTRATIONS	50
	5.4	SUMMARY	51
6.	**THE EFFECT OF SOLUTION CONCENTRATION, CARBON LOADING, SLURRY DENSITY, STIRRING SPEED AND CARBON CONCENTRATION ON ADSORPTION KINETICS**		**56**
	6.1	THE GOLD ADSORPTION PROFILE	57
	6.2	SLURRY DENSITY AND STIRRING SPEED VERSUS POWER CONSUMPTION	58
	6.3	CONSTANT RATE PERIOD	58
	6.4	TURNING POINT	59
	6.5	DIMINISHING RATE PERIOD	59
	6.6	SUMMARY	60
7.	**CONCLUSIONS**		**73**

8. FUTURE WORK 75

NOMENCLATURES 77
REFERENCES 79
APPENDIX A RAW DATA FROM STIRRING SPEED EXPERIMENTS 87
APPENDIX B RAW DATA FROM ISOTHERM EXPERIMENTS 89
APPENDIX C RAW DATA FROM BATCH EXPERIMENTS 91

LIST OF TABLES

		PAGE
Table 1.1	The various types of elution processes available, along with their advantages and disadvantages.	26
Table 1.2	The various types of electrowinning cells available.	27
Table 5.1	K_f values for densities 1100, 1300 and 1500 kg.m^{-3} at a constant stirring speed of 520 rpm.	52
Table 5.2	K_f values for stirring speeds of 450, 520 and 590 rpm at a constant density of 1300 kg.m^{-3} .	53
Table 6.1	The effects of initial concentration, mixing and "blinding" on the constant rate period.	67
Table 6.2	The goodness of fit of the predicted values to the experimental data for the constant rate period	68
Table 6.3	The effects of initial concentration on the turning point.	69
Table 6.4	The goodness of fit of the predicted values to the experimental data for the "turning point".	70
Table 6.5	The effects of solution concentration, carbon loading, mixing and "blinding" on the diminishing rate period.	71
Table 6.6	The goodness of fit of the predicted values to the experimental data for the diminishing rate period.	72

LIST OF FIGURES

		PAGE
Figure 1.1	A schematic representation of the structure of graphite.	28
Figure 1.2	A schematic representation of the proposed structure of activated carbon.	29
Figure 1.3	An illustration of the pore structure of activated carbon.	30
Figure 1.4	A flow diagram representing the Carbon-in-Pulp circuit.	31
Figure 3.1	The apparatus for experiments performed in 1 L reactors.	41
Figure 4.1	A graphical representation of the linear form of the Linear isotherm.	44
Figure 4.2	A graphical representation of the linear form of the Freundlich isotherm.	45
Figure 4.3	A graphical representation of the linear form of the Langmuir isotherm.	46
Figure 4.4	A graphical representation showing how the predicted Qe vales of the Freundlich, Langmuir and Linear isotherms fit the experimental data.	47
Figure 5.1	A graphical representation of the K_f values for densities 1100, 1300 and 1500 $kg.m^{-3}$ at a constant stirring speed of 520 rpm.	54
Figure 5.2	A graphical representation of the K_f values for stirring speeds of 450, 520 and 590 rpm at a constant density of 1300 $kg.m^{-3}$.	55
Figure 6.1	A graphical representation of the various sections of a gold adsorption profile.	62
Figure 6.2	A graphical representation of the exponential relationship between minimum stirring speed and slurry density.	63
Figure 6.3	A graphical representation of Reynolds number versus power number.	64
Figure 6.4	A graphical representation of the effects of changing density on the gold adsorption rate during the constant rate period.	65

Figure 6.5 A graphical representation of the effects of percentage changes in solution concentration and carbon loading on the gold adsorption rate. 66

Figure 8.1 A flow diagram of the proposed computer package. 76

CHAPTER 1

INTRODUCTION AND LITERATURE STUDY

Activated carbon is used extensively to recover aurocyanide from solution in the gold mining industry. In this study the adsorption rate onto activated carbon under varying operating conditions was investigated. The effects of carbon concentration, gold concentration, slurry density and agitation rate were evaluated using linear regression techniques.

1.1 ACTIVATED CARBON

Activated carbon is a generic term for a family of highly porous carbonaceous materials, none of which can be characterised by a structural formula or chemical analysis *[McDougall, 1981 & 1991]*.

1.1.1 Raw Materials

Activated carbons are produced from a wide variety of raw materials, including peat, peach pits, wood char, bone char, coconut shells, carbon black, etc. *[Balci et al., 1994; Bhappu, 1990; McDougall, 1991; Mattson et al., 1971]*. The choice of raw material along with the method of production, has a large effect on the structure and properties of the end product *[Bailey, 1971; van Dam, 1995]*. Activated carbons are commercially available in a powdered or granular form. The granular form comes in various sizes and shapes. Moreover, these shapes are either natural or moulded into rods, 0.8-6 mm in diameter and 3-10 mm in length *[McDougall, 1991]*.

1.1.2 Physical Manufacturing

1.1.2.1 Carbonisation

Carbonisation involves the gaseous pyrolysis of the starting material to drive off the non-carbon elements (H, O, traces of S and N), leaving a product consisting of around 90% carbon *[de Jong, 1991; Mattson, 1971]*. Pyrolysis requires an inert atmosphere (absence of air) without the addition of chemical agents *[Balci et al., 1994; Hassler, 1974]*. Although temperatures in the range of 300 - 600°C are preferred, it is not uncommon to see temperatures as high as 900°C as in the case of sugar *[Bailey, 1971; McBain, 1936]*. The product of carbonisation is a hydrophobic skeleton which is made up of an irregular crystalline structure with free fissures remaining between the crystallites *[Bailey, 1987]*. However, the decomposition and deposition of disorganised carbon results in the filling or blocking of these pores. An activation step is therefore necessary to enhance the low adsorption capacity of the carbon *[Balci et al., 1994]*.

1.1.2.2 Activation

Activation involves the partial gasification of the carbon in the presence of oxidising agents (steam, carbon dioxide or air). The reactive oxygen burns away parts of the carbon skeleton, resulting in its release as CO and CO_2 *[Bailey, 1971; Balci, 1994; McDougall et al, 1981]*. Temperatures in the range of 700-1000°C are used which facilitate controlled dehydration and devolatilization of parts of the carbon *[Bailey, 1971; Hassler, 1974; McDougall, 1991]*. In creating carbon with a large adsorptive capacity, conditions are created under which the activation reagent reacts with the carbon, and activation becomes a two stage process *[Ibrado, 1992]*:

- the first stage involves the burn-off of the disorganised carbon which blocks the pores, with no more than 10-20% burn-off being obtained.
- the second stage involves further activation of the carbon and burn off of elementary crystallites

Due to the low affinity of dicyanoaurate for chemically produced products, the thermal manufacture of activated carbon has become the preferred route for the production of products suitable for use in the gold-recovery process *[McDougall, 1991].*

1.1.3 Chemical Manufacture

Although the majority of activated carbon is produced by the physical process of steam activation, a number of chemical alternatives are available. Chemical activation is used mainly for uncarbonized cellulose materials, primarily wood *[McDougall, 1991].* The most commonly used chemical activating agents include zinc chloride, phosphoric acid and salts of sodium and magnesium *[Balci, 1994; Hassler, 1974].*

Initial stages involve the mixing of the raw material with a dehydrating agent (Sodium carbonate, sodium and calcium hydroxide, etc.). The resulting mixture is dried at temperatures in the range of 200-650°C which results in the formation of a carbon skeleton. Activating agents are then added and this mixture is then heated to 350-650°C *[McDougall 1991].*

As the temperatures required are lower than those needed for physical activation, smaller crystallites are formed which promote the development of the pore structure *[de Jong, 1991].* Chemically activated carbons are characterised by their generally macroporous structure making them suitable for the adsorption of large molecules*[McDougall; 1991].*

1.1.4 Physical Structure of Activated Carbon

The most important physical properties of activated carbon are: the number and size distribution of the pores, bulk density, dry impact hardness, wet abrasion resistance and particle-size distribution *[McDougall, 1991].* However, there are three properties common to all types of activated carbon which best describe its high adsorptive ability*[Ibrado, 1992]*:

- a large specific surface area

- a partially oxidised surface
- a charred (carbonised) organic substrate

X-ray studies have shown activated carbon to have a structure similar to that of graphite *[Hassler, 1974; Mattson, 1971; McDougall, 1991].* As can be seen in Figure 1.1, graphite consists of fused hexagonal rings forming layers which are held approximately 3.35 Å apart by Van der Waals forces *[McDougall, 1991].* Thermally activated carbons are believed to be made up of tiny graphite-like platelets only a few carbon atoms thick and 20 to 100 Å in diameter (See Figure 1.2). They form the walls of open cavities or pore structures. As the hexagonal carbon rings are randomly arranged and many have undergone cleavage, the overall structure is very disorganised. The separation between the layers is also greater than that of graphite, i.e. 3.6 Å *[de Jong, 1991; McDougall, 1991].*

The pore structure and surface area of activated carbon is developed during the carbonisation and activation processes. Although the pores are usually cylindrical or rectangular, they can occur in a variety of shapes. Pores can be classified according to three distinct groups based on their pore diameter*[Bailey, 1971; de Jong, 1991; McDougall, 1991]*:

- macropores (> 25 nm), are channels which are determined by the cell structure of the original carbon material. They provide rapid access to the meso- and micropores where actual adsorption takes place.
- mesopores or transitional (1-25 nm and account for 5% of the internal surface area), are situated between graphite-like micro-crystallites which are also formed by activation perpendicular to the plates.
- micropores (< 1 nm and account for 95% of the internal surface area), are developed during activation, when graphite-like micro-crystallites are affected.

(Figure 1.3 gives an illustrated representation of the pore structure of activated carbon)

The carbon-in-pulp and carbon-in-leach processes make considerable use of coconut-shell activated carbons. This is due to their good impact hardness and wet abrasion resistance *[Dahya, 1983; Laxen et al, 1994; Yannopoulos, 1990]*, coupled with a large capacity for small gold dicyanoaurate complex adsorption due to an extremely microporous structure *[Beaty, 1994; McDougall, 1991]*.

1.1.5 Chemical Properties of Activated Carbon

Due to the structural imperfections there are many opportunities for reactions with carbon atoms forming the edges of the planar layers. These reactions result in the formation of oxygen-containing functional groups on the surface of the carbon *[Mattson, 1971; McDougall, 1991]*. Although a large number of these groups have been identified (carboxyl, penolic hydroxyl, quinon-type carbonyl, normal lactones, fluorescein, carboxylic acid anhydrides and cyclic peroxides), carbon remains unamendable to infrared spectroscopy, leaving doubts as to the nature of unidentified groups *[McDougall, 1980]*. It is however known that the nature of the surface groups are dependent on the conditions during and after manufacture *[Mattson, 1971; McDougall, 1991]*.

1.2 GOLD BEARING ORES

Cyanidation remains the most effective and widely used process for the leaching of gold and silver from their ores *[Adamson, 1972; Yannopoulos, 1991; Young, 1987]*. However, certain ores require pre-treatment to make this process economically viable, and in some cases possible. Gold bearing ores can therefore be divided into free milling and refractory ores.

1.2.1 Free milling ores

These ores give a recovery rate of more than 88% when subjected to conventional 20-30 hour cyanidation leaching. They consist of sulphide and oxide ores, which require no additional pre-treatment after milling *[La Brooy, 1994; Yannopoulos, 1991; Bhappu, 1990].*

1.2.2 Refractory ores

These ores yield poor gold recoveries, usually less than 80% by standard cyanidation processes. The reasons for poor recovery may be chemical or physical in nature.

Chemical:
- insoluble gold tellurides
- cyanicides or cyanide consuming ores (pyrrhatite, covellite, etc.)
- oxygen consuming ores (sulphide ions, ferrous ions, etc.)

Cyanicides and oxygen consumers will cause precipitation of gold from solution.

Physical:
- attached or encapsulated gold (pyrite, arsenoyrite, silica)
- gold alloys (Sb, Pb, etc.)
- gold coated with a film (iron oxide, silver chloride, etc.)
- gold pregrobbed from solution (carbonaceous materials and clay)

[La Brooy, et al, 1994; Petruk, 1989; Wang, 1990; Yannopoulos, 1991]
As a result of the gradual depletion of high grade and free milling ores, it became necessary to investigate the processing of refractory ores. Pre-treatment processes were developed which facilitate higher gold recovery by cyanidation *[Bhappu, 1990; La Brooy, et al, 1994; Yannopoulos, 1991]*:

- thermal treatment (roasting)
- pressure oxidation (acid or alkaline)
- chemical treatment

- biological treatment
- physical treatment (finer grinding)

1.3 CARBON-IN-PULP CIRCUIT (CIP)

The carbon-in-pulp (CIP) circuit was first employed on a small scale by the Carlton Mill around 1951 *[Fast, 1988]*. However, it was only in August 1973 that the process gained recognition when the first large scale CIP circuit was commissioned by the Homestake Mining Company *[Hall, 1974]*. The CIP circuit has since become the preferred route for gold recovery. Figure 1.4 shows a schematic layout of a typical CIP circuit. The reasons for its popularity are*[Bailey, 1987; Stanely, 1990]*:

- reduced capital expenditure
- reduced operating costs
- improved gold recovery
- reduced sensitivity of recovery to throughput rate
- ability to handle shaley and clayey ore more efficiently than filtration

The mined ore first undergoes crushing and grinding to obtain a particle size of 80% under 75μm *[La Brooy et al, 1994]*. As water is added during grinding, a thickener is necessary to obtain the correct solid: liquid ratio prior to cyanidation *[Adamson, 1972; Bailey, 1987; Stanley, 1990; Yannopoulos, 1991]*. Cyanidation involves the contacting of gold bearing ore with a cyanide solution to leach the gold from the ore.

1.3.1 Adsorption

After cyanidation the ore pulp is pre-screened at 710 μm before it enters the CIP circuit. This facilitates the removal of wood chips or other oversized materials which may block the interstage screens*[Bailey, 1987; Dahya, 1983; Laxen et al, 1994; Menne, 1982]*. Adsorption

takes places in a series of six to eight agitated tanks. These tanks are arranged in a cascade to facilitate the use of gravity for continuous movement of the pulp *[Bailey, 1987; Yannopoulos, 1990]*. The slurry is then contacted with the activated carbon, which is moved intermittently and in a countercurrent direction to the pulp. Therefore, the solution gold value decreases downstream, while the loaded gold value on the carbon increases upstream *[Bailey, 1987; Dahya, 1983; Laxen et al, 1994]*. The pH of the pulp is maintained in the range of 10-11 through the addition of lime *[Yannopoulos, 1990]*.

1.3.1.1 Tank size and layout

The size and number of adsorption tanks depend mainly on the feed gold concentration. The number of tanks increases with higher initial gold concentrations *[Laxen et al, 1994]*. Furthermore, the tank size must be sufficient for a retention time of one hour, although larger plants work with longer retention times. These tanks have a staggered layout, with heights between tops of tanks varying with 0.3-1 m. Open launders or pipes are used to interconnect the tanks in order to facilitate the flow of the ore pulp *[Bailey, 1987]*.

1.3.1.2 Mixing

Mixing remains an important design consideration, as incorrect design and operation can result in major gold losses. This is due to the production of carbon fines and the imperfect contacting of the carbon and pulp mixture *[Dahya, 1983]*.

Mixing can be performed using either mechanical or air agitation. Mechanical agitation remains the more popular choice as its adsorption kinetics are twice as high as air agitation *[Menne, 1982]*. In the case of mechanical agitation, draught-tube circulators are fitted with slitted skirts and are preferred over the standard baffled tanks with shrouded impellers. Moreover, the draught-tube circulators clear settled solids more effectively during start-up after power trips. However, draught-tube circulators are ineffective for slurries with a relative

density lower than 1.3. These high densities are required for satisfactory operation and to ensure faster-settling particles do not segregate and settle *[Dahya, 1983; Menne, 1982].*

1.3.1.3 Interstage screening

Interstage screens are installed to ensure separation of carbon and pulp on a size basis. This allows for continuous flow of pulp down the adsorption train while retaining the activated carbon which is moved intermittently from tank to tank up the adsorption train [Dahya, 1983; Yannopoulos, 1990]. There are two types of interstage screens used in industry *[Dahya, 1983, Yannopoulos, 1990]*, namely:

- Airswept static screens with the pulp airlifted onto external screens which allow the pulp to pass through while retaining the carbon and returning it to the same tank.
- Equalised-pressure air cleaned (EPAC) screens which are placed on the periphery of the tank. These provide minimal blockage as long as the pulp levels on either side of the screen are maintained as near to equal as possible.

1.3.1.4 Carbon transfer

Carbon transfer is dependent mainly on the dissolved gold fed to the circuit and gold loading on fully loaded carbon. Less frequent movement of carbon results in higher loading on carbon in each stage. Carbon transfer is effected by use of airlifts or pumps. The choice of transport method is dependent mainly on the size of the plant. Pumps are used mainly for large scale plants *[Laxen et al, 1994; Menne, 1982].*

Carbon transfer can be done on a continuous or intermittent bases *[Stange et al, 1990].* The time taken for carbon transfer is dependent on the capacity of the pumps used, the concentration of the carbon and the means of transfer *[Stange et al, 1990].* When considering the duration of transfer times it should be noted that a single large transfer is more effective than a number of smaller transfers *[Bailey, 1987].* It should also be noted that the amount of carbon transferred

daily is not constant and that carbon transfer is not an instantaneous process. As a result of these variations steady-state is never reached *[Schubert et al, 1993; Stange et al, 1990]*.

1.3.2 Elution

It was not until 1952 that Zadra developed a technique for stripping the loaded carbon using a hot sodium hydroxide-sodium cyanide solution. This process was effective for elution of both gold and silver and produced carbon which remained reasonably active for 10 to 15 cycles *[Laxen et al, 1994, Zadra et at, 1952]*. The long stripping time required for this process remained a problem and further investigation led to the development of processes with shorter stripping time. In an attempt to optimise the elution process variations in stripping solutions and operating conditions were investigated resulting in the development of additional techniques. Four elution techniques are in common use. These are given along with there advantages and disadvantages in Table 1.1 *[Bailey, 1987; Dahya et al, 1983; Laxen et al, 1982 & 1994; Stange, 1991; Wan et al, 1990; Yannopoulos, 1991]*.

All elution processes are based on Ficks First Law:

$$J = -\frac{DC}{R_g T} \cdot \frac{d\mu}{dy} \qquad (1.1)$$

where, mass transfer rate is a linear function of the molar concentration gradient (high temperature) *[Coulson and Richarson, 1990]*

1.3.3 Carbon Regeneration

During the CIP process various organic and inorganic species are adsorbed onto the carbon. These impurities cannot be removed during elution and cause excessive poisoning and loss of activity *[Bailey, 1987; Dahya, 1983; Yannopoulos, 1991]*. It is therefore necessary for the carbon to undergo regeneration, the frequency of which is dependent on the type of ore used.

Thermal regeneration involves heating the carbon to 650°C in the absence of air for 30 minutes *[Bailey, 1987; Dahya, 1983; Laxen et al, 1994; Yannopoulos, 1991]*. This is done by introducing wet carbon into a rotary kiln, the feed end of which is sealed to force the steam generated to pass over the carbon bed. The steam is then exhausted from a flue pipe at the discharge end and so prevents air from entering the kiln *[Dahya, 1983; Yannopoulos, 1991]*. However, regeneration results in the partial combustion of the carbon (carbon losses due to combustion increases with time and activation temperature) as expressed in equations 1.2 and 1.3 *[Bailey, 1987; Dahya, 1983; Yannopoulos, 1991]*:

$$C + H_2O \rightarrow CO + H_2 \qquad (1.2)$$

$$C + 2H_20 \rightarrow CO2 + 2H_2 \qquad (1.3)$$

Reactivated carbon is then air cooled in the cooling section of the kiln or in a hooper. The reactivated carbon is then screened at 20 mesh to remove fines and conditioned with water before recycling to the adsorption circuit *[Bailey, 1987; Dayha, 1983]*.

1.3.4 Electrowinning

Electrowinning remains the most widely used method for the recovery of gold from eluted solutions. Table 1.2 describes a number of the cells which have been designed for this purpose *[Bailey, 1987; Dahya, 1983]*. The majority of these cells contain a steel wool cathode. This is due to the large surface area it provides for electrolytic deposition of precious metals *[Dahya, 1983; Laxen et al, 1994]*. These cathodes are capable of loading 30 kg of gold and 6 kg of silver, after which they are removed and smelted with a flux (borax, niter, and silica) to produce a high purity bullion *[Bhappu, 1990; Laxen et al, 1994]*. In some cases the removed cathodes are dissolved in hydrochloric acid and the residue is then smelted. This process reduces the consumption of flux during smelting *[Dahya, 1983]*.

1.4 MECHANISMS FOR GOLD CYANIDE ADSORPTION

Over the years a number of possible mechanisms have been suggested for the adsorption of dicyanoaurate onto activated carbon. However, no consensus has been reached and all possible mechanisms can be simplified into one of three basic forms:

- The $Au(CN)^{2-}$ ion is adsorbed without undergoing chemical change, and held by electrostatic or Van der Waals forces,
- The gold compound is decomposed from $Au(CN)^{2-}$ to Au(CN) and adsorbed as such,
- The aurocyanide is reduced to either gold metal or to a partially reduced state between gold(I) and gold(0).

[Adams et al, 1989; Jones et al, 1989; McDougall et al, 1980; Wan et al, 1990; Yannopoulos, 1990]

Doubts surrounding the mechanism for adsorption stem mainly from the fact that carbon is not amendable to infrared spectroscopy or any other technique of physical investigation *[McDougall, 1980].* This makes it difficult for investigators to know the true nature of the oxygen containing functional groups on the carbon which play an important role during adsorption.

1.5 FACTORS AFFECTING GOLD CYANIDE ADSORPTION

1.5.1 Cyanide Concentration

Free cyanide has a negative effect on the gold loading onto activated carbon. This may be due to its large effect on the selectivity of carbon for gold adsorption. The following factors affect the free cyanide concentration in solution:

- Carbon concentration: Although free cyanide losses do occur in the absence of activated carbon, this is a slow process. However, in the presence of activated carbon, the cyanide undergoes catalytic oxidation to cyanate. The carbon then acts as a catalyst for decomposition of the cyanate. In addition, some of the cyanide and cyanate are adsorbed by the carbon.
- Temperature: The cyanide losses in the presence of activated carbon are enhanced by high temperatures.
- pH levels: pH levels above 10 result in no significant losses, while lower pH levels account for considerable cyanide losses. This effect can be explained by the presence of copper (which is found in most gold mining slurries) at lower pH levels, due to the reduced copper loading. Copper promotes the hydrolysis of cyanides to bicarbonate and ammonia.
- Free oxygen content: Oxygen in its molecular form acts as an oxidant for the oxidation of cyanide to cyanate in the presence of activated carbon.

[Adams, 1990: Bailey, 1987; Davidson, 1986, Davidson et al 1982; Yannopoulos, 1990].

1.5.2 Gold and Carbon Concentration

An increase in gold concentration in solution has a positive effect on adsorption rate due to the increased diffusion gradient between the solution and carbon surface. Although there is an increase in adsorption rate the increase in solution concentration has no effect on the equilibrium loading of the carbon. The carbon concentration in adsorption vessels is usually maintained in the range of 15 to 40 $g.l^{-1}$ *[Yannopoulos, 1990].*

1.5.3 pH

An increase in pH has a negative effect on the rate of aurocyanide adsorption onto activated carbon *[Adams, 1989; McDougall, 1980; Petersen, 1991; Yannopoulos, 1990].* This drop in adsorption rate can be explained by the competition of hydroxide and aurocyanide ions for

active sites on the carbon. Although lower pH levels provide higher adsorption rates, the pH of 10.5-11 is maintained for safety purposes.

Carbon-in-pulp circuits make use of lime to raise the pH of the slurries. The high pH caused by the increased hydroxide ions has a decreasing effect on gold adsorption, while the calcium cations enhances the gold adsorption. Therefore, it can be said that lime addition has very little effect on the gold adsorption *[Yannopoulos, 1990]*.

1.5.4 Temperature

An increase in the temperature at which adsorption takes place will have a negative effect on the adsorption rate. This is due to the exothermic nature of the reaction *[Bailey, 1987; Davidson, 1974]*. However, the change in ambient temperature caused by heat released from this exothermic reaction has insignificant effects on the adsorption process *[Davidson, 1974; Woollacott et al, 1993]*. Furthermore, the solubility of the aurocyanide in hot water is considerably higher than that in cold water *[McDougall et al, 1980]*.

1.5.5 Free Ions (Ionic Strength)

An increase in the free ion content of the adsorption solution has an enhancing effect on both the adsorption loading capacity as well as the adsorption rate. However, the effect on the loading capacity is much greater than that on the adsorption rate. The following series shows the order of ionic strength of the following cations *[Davidson, 1974]*:

$$Ca^{2+} > Mg^{2+} > H^{+} > Li^{+} > Na^{+} > K^{+}$$

Earlier researchers believed that the increase in adsorption rate was due to the increased ionic strength of the solution *[Davidson, 1974]*. However, two flaws were found in this argument*[Bailey, 1987; McDougall, 1980]*:

- Tests were performed using three times more KCl than $CaCl_2$ and it was discovered that the KCl did not provide loading enhancement anything near that of the $CaCl_2$.
- The dramatic loading enhancements obtained when small additions of electrolyte were added was not in keeping with the simple ionic strength effect.

These experiments proved that it is the charge of the cation and not its size that enhances the adsorption of gold. Furthermore, one is forced to conclude that divalent cations are specifically involved in adsorption.

1.5.6 Particle Size

A decrease in particle size, for the same mass of carbon, increases the adsorption rate, while having no effect on equilibrium loading. This is due to the increased surface area provided by the smaller particles *[Bailey, 1987; Fleming et at, 1984; Yannopoulos, 1991]*. Fleming et al *[1984]*, showed experimentally that gold adsorption onto carbon with mean diameters in the range on 0.42-2.38 mm is controlled by film diffusion. The adsorption rate in these experiments were inversely dependent on the mean particle diameter, unlike the inverse squared dependency displayed by rates controlled by particle diffusion *[Bailey, 1987; Fleming et al, 1984]*. However, it should be noted that inclusion of particles smaller than 1 mm could provide problems during pulp screening *[Bailey, 1987]*.

1.5.7 Pulp Density

An increase in pulp density has a negative effect on the adsorption rate. This could be due to the following factors*[Jones et al, 1989; Petersen et al, 1993]*:

- The temporary blinding of the exposed carbon surface.
- The partial blockage of the carbon pores with ore particles. This slows the rate of the reaction but does not affect the eventual access to the pores after extended lengths of time.

- Stirring speeds in the range of 250-1500 rpm affect the rate constant (k). This indicates that solution mass-transport controls the gold adsorption reaction below 1500 rpm. An increase in stirring rate in this range increases the adsorption rate.
- Increased viscosity makes mixing conditions more difficult. Little change would be expected when there are 0-30% solids present. However, at concentrations higher than 30% solids the effects should be noticeable.

The pulp density limits are important for intermixing of the carbon with the ore suspension. If solids make up less than 40% of the pulp the carbon tends to sink. If the pulp is more than 45%, the carbon floats *[Yannopoulos, 1991]*.

1.6 NON-IDEAL CONDITIONS

1.6.1 Back-mixing

As mentioned earlier, carbon transfer takes place using one of two methods; continuous or intermittent transfer *[Stange et al, 1990]*. This transfer is not an instantaneous process which results in the carbon in the different tanks becoming mixed during the transfer *[Stange, 1991; Woollacott et al, 1992]*.

Furthermore, the screening units used are also imperfect, resulting in the leakage, and therefore co-current movement of carbon. Other factors which contribute to this occurrence are carbon breakage, screen overflow and passage of platelet shaped carbon particles through the slots in wedgewire screens *[Schubert et al, 1993; Stange et al, 1990; Woollacott et al, 1990]*. Back-mixing is one of the main contributing factors to gold lock-up.

1.6.2 Gold lock-up

A factor which adds significantly to gold lock-up is the seepage of finer carbon particles through the interstage screens. These finer particles adsorb and desorb gold at a very rapid rate and therefore adsorb gold in the more concentrated solutions. As they move co-currently to the slurry they come into contact with solutions of lower gold tenor which results in desorption of adsorbed gold. This adsorption and desorption of gold by these particles therefore result in the cycling of substantial amounts of gold throughout the carbon train, resulting in much of this gold remaining in the adsorption circuit *[Schubert, 1993]*.

1.6.3 Carbon breakage

Carbon attrition results from the collision of the carbon particles with other carbon particles, the ore particles or parts of the tank equipment. This process can take place on a wet or dry base, with dry carbon attrition usually occurring during reactivation and dry screening. Although carbon attrition is very complex, all attrition types involve two basic mechanisms*[van Dam, 1993]*:

- carbon abrasion - the carbon particles are rubbed against the ore particles, other carbon particles, or parts of the tank equipment, resulting in their gradual decrease in size.
- carbon fragmentation - the carbon particles are subjected to a high enough impact force, which results in small pieces of the particle being chipped away.

Although carbon abrasion takes place as a result of collisions with the ore and equipment, no connection has been found between the rate of carbon consumption, type of ore, and equipment being used *[Sorensen, 1989]*. Furthermore, an equilibrium must be reached between the degree of activation and the impact hardness of the carbon. The more the carbon is activated the less resistant it becomes to abrasion wear *[van Dam, 1995]*.

Carbon abrasion accounts for a substantial amount of the gold losses experienced in the CIP circuit. This is due to the finer carbon particles leaking through the interstage screens and therefore move co-currently to the pulp and leave the circuit with the barren solution *[Schubert, 1993]*.

1.6.4 Competitive adsorption of other species

Gold bearing ores contain a number of additional metallic elements in the form of oxides, sulphides, arsenides, or antimonides. Some of the metallic elements present are: copper, nickel, cobalt, iron, and zinc. As these metals are at least partially soluble in cyanide they form metal-cyanide complexes during the cyanidation process. These metal-cyanides can then cause problems in the CIP circuit when they are absorbed onto the activated carbon along with the gold. However, it must be noted that gold will load in preference, followed by copper. No sequence is available for the order of adsorption of the other complexes onto the activated carbon. This is due to the sensitivity of their adsorption to processing parameters such as: pH, free cyanide concentration, temperature and their concentration in the leached slurry. Although these other metals are adsorbed, they are at very low concentrations and do not cause serious problems *[Bailey, 1987; Fleming et al, 1984; Yannopoulos, 1991]*.

It can therefore be said that the only metal-cyanide complex which plays any significant role in the gold adsorption process is copper. This is due to its ability to oxidise free cyanide present in the solution. The reduction in free cyanide concentration enhances gold adsorption onto the carbon *[Bailey, 1987; Fleming et al, 1984]*.

1.6.5 Circuit foulants

Foulants in the adsorption circuit can be inorganic or organic in nature and cause a decrease in not only the adsorption rate, but also the equilibrium loading of the gold onto the carbon *[Liebenberg et al, 1997]*. There are a number of possible explanations for these effects, namely *[Bailey, 1987; Fleming et al, 1984; Petersen et al, 1991]*:

- foulants are adsorbed into the pores, partially blocking them
- the formation of a film barrier of the compound around the carbon particle
- the solvation of the gold cyanide ions by these compounds, therefore reducing the gold concentration in solution

Inorganic foulants include rust, slimes, etc *[Laxen et al, 1979 & 1982]*. Smith et at (1984), concluded from the results of fouling tests that the presence of dissolved inorganic matter plays only a small role in the deactivation of the carbon, and that organic foulants pose the greater concern. Organic foulants have a number of sources, the main ones being*[La Brooy et al, 1986]*:

- mining chemicals present as a result of addition or spillage during mining, milling, flotation, and equipment maintenance.
- some foulants are present in the ore itself or in process water, derived from rotting timber, plants and sewage.
- chemicals left on the carbon as a result of gold desorption techniques

Although these foulants pose problems in the adsorption circuit they can easily be removed by thermal regeneration *[La Brooy et at, 1986]*.

1.6.6 Wood chips

Wood chips are formed by the degradation of the timber used for roof supports in underground mines. These wood chips cause a number of problems in the circuit *[Bailey, 1987; Minson, 1986; Sorensen, 1989]*:

- They blind or block the interstage screens, causing the pulp and loaded carbon to flow over the screens. This flattens the carbon activity profile and the efficiency of the gold adsorption is reduced.

- The clean carbon flows easily, whereas the carbon which becomes mixed with wood chips has poor flow characteristics.
- The oversized particles take up space in the adsorption tanks, leading to lower than designed pulp residence times in the adsorption tanks. This causes poor stripping of carbon and the lowering the residual gold loading on the carbon when it is returned to the circuit. The result is lower adsorption efficiency and loss of dissolved gold to residue.

1.6.7 Pregrobbing

Pregrobbing involves the adsorption of gold by other gold adsorbing species in the slurry. Two of the main culprits are; silica or various types of quartz ore and wood chips.

1.6.8 Non-ideal mixing and retention time

The assumption which is often made during attempts to optimise the CIP circuit is that the tanks in the train are well mixed. This implies that the gold tenor of the slurry inside the tanks and that leaving the tanks are the same. However, this is not the case, as substantial amounts of the slurry bypass or short-circuit to the outlet of the tanks in less time than the mean residence time of the tank *[Woollacott et al, 1990]*.

Furthermore, the amount of carbon transferred per day varies. This, along with back-mixing, results in an unsteady-state in the adsorption train *[Stange, 1990]*.

1.7 ADSORPTION MODELLING

Many attempts have been made to model the carbon-in-pulp process. One of the first developed models used originated from the Fairview pilot plant [*Fleming et al, 1979*]. This rate expression model was used for the pilot plant at Grootvlei which, however, resulted in an over-design. It was concluded that the order dependent on time was different at the two mines. This

work resulted in the "kn" model and is the rate equation most commonly used for the design of carbon-in-pulp plants.

$$\frac{C_s(I)}{C_s(i)} = \left[1 + k\left(\frac{M_c}{F_c}\right)^n x \frac{F_c}{F_s}\right]^i$$

Where:	Cs(I)	-	concentration of gold in incoming solution	($mg.l^{-1}$)
	Cs(I)	-	concentration of gold in solution in stage I	($mg.l^{-1}$)
	k	-	rate constant	(h^{-1})
	Mc	-	mass of carbon	(tons)
	Fc	-	flow rate of carbon	($tons.h^{-1}$)
	Fs	-	flow rate of solution	($m^3.h^{-1}$)
	n	-	order of reaction	($tons.h^{-1}$)
	i	-	stage number	

This model is relatively simple in that only two parameters need to be determined. However, the mechanism for adsorption changes from film to intraparticle diffusion as loading increases and applying a single rate model as the one above over the whole spectrum of adsorption could result in significant errors.

To overcome this problem a branched pore model was developed by van Deventer [*van Deventer*, 1986]. This model does describe the changing mechanism but was carried out using solutions of pH 8.5, rather than using plant conditions of pH between 11 and 12. Also, the model is mathematically complex and a number of parameters must be determined or estimated. This model is described in Chapter 2.

1.8 LINEAR REGRESSION

Linear regression involves the study of the dependency of one variable on one or more other variables with the view to estimating and/or predicting the mean or average value of the formers in terms of the known or fixed values of the latter. The relationships derived in this study were obtained by the method of ordinary least squares (OLS estimation).

1.8.1 Linear regression terms

The relationships that exist between the explanatory and dependent variables can be described by equations in the following form:

$$Y = \beta_1 + \beta_2 X_{2i} + \beta_3 X_{3i} \ldots + \beta_n X_{ni} + u_i \qquad (1.2)$$

Where:

	Y	The dependent variable
	$X_{2,3,4}$	The explanatory variables
	$ß_{2,3,4}$	The regression coefficients

These relationships are derived using OLS estimation when the following assumptions are made:

- The mean value of u_i is zero
- No autocorrelation exists between the u-values
- Equal variance of u_i (homoscedasticity)
- Zero covariance between u_i and any of the explanatory variables (X variables)
- No exact linear relationship among the explanatory variables (no multicollinearity)

1.8.2 Matrix approach to linear regression

A matrix is an array of numbers that can be used to present or summarise business data. Equation (1.2) can be converted to matrix notation:

$$\begin{bmatrix} Y_1 \\ Y_2 \\ \cdots \\ \cdots \\ Y_N \end{bmatrix} = \begin{bmatrix} 1 & X_{21} & X_{31} & \cdots & \cdots & X_{n1} \\ 1 & X_{22} & X_{32} & \cdots & \cdots & X_{n2} \\ \cdots & \cdots & \cdots & \cdots & \cdots & \cdots \\ \cdots & \cdots & \cdots & \cdots & \cdots & \cdots \\ 1 & X_{2N} & {}_{3N} & \cdots & \cdots & X_{nN} \end{bmatrix} \times \begin{bmatrix} \hat{\beta}_1 \\ \hat{\beta}_2 \\ \cdots \\ \cdots \\ \hat{\beta}_5 \end{bmatrix} + \begin{bmatrix} e_1 \\ e_2 \\ \cdots \\ \cdots \\ e_N \end{bmatrix}$$

Or $Y = X\hat{\beta} + e$

The βeta-Array is then determined using the following equation:

$$\hat{\beta} = X' X^{-1} \cdot Y' X \qquad (1.3)$$

Where: X' is the transpose of X, where transpose infers the interchanging of the rows and columns in a matrix.

X^{-1} is the inverse of X, the inverse being a unique matrix that may be multiplied by the original to create an identity matrix. An identity matrix being a square matrix with 2's on its diagonal and 0's in all the other positions.

The R^2 value is determined using the equation:

$$R^2 = \frac{\hat{\beta} X' y - N\overline{Y}^2}{y' y - N\overline{Y}^2} \qquad (1.4)$$

Where: R^2 is a measure of the proportion or percentage of the total variation in Y explained by the regression model (The goodness of fit of the model). The R^2 value lies between 0 and 1.

$\hat{\beta}$ the array of regression coefficients

N the number of X-data readings

1.8.3 Irregularities in linear regression

1.8.3.1 Heteroscedasticity

Heteroscedasticity can best be explained by first explaining the term homoscedasticity. Homoscedasticity is one of the important assumptions of the classical linear regression model. It assumes that the variance of each disturbance term u_i, conditional on the chosen values of the explanatory variables, is some constant number equal to σ^2. Heteroscedasticity is a situation during which this assumption is not satisfied.

1.8.3.2 Multicollinearity

Multicollinearity is the existence of either an exact or approximately exact linear relationship among all or some of the explanatory (or X) variables of a regression model.

1.8.3.3 Autocorrellation

Autocorrellation is a violation of the assumption that the errors or disturbances u_i entering the population regression function are random or uncorrelated.

1.9 OBJECTIVES

From the literature study it is clear that an abundance of information is available on activated carbon, aurocyanide adsorption onto activated carbon, carbon-in-pulp operations and modelling of adsorption onto carbon black. However, grey areas exist on the combined effects of operating parameters such as agitation rate and slurry density on the adsorption of aurocyanide onto activated carbon. Furthermore, the models available to predict CIP

performance or adsorption rate are either complex in nature or provide estimates with a high degree of uncertainty. In this study linear regression techniques will be used in an attempt to not only predict adsorption rate accurately but also to incorporate operating parameters such as slurry density and agitation rate.

Name of process	Conditions under which process operates	Advantages and disadvantages
Zadra	• NaOH and 0.1% NaCN • 85-95°C • atmospheric pressure • 24-60 hours	Advantages : • relatively low capital cost Disadvantage: • long cycle time is a limiting factor on large scale plants
Anglo American (AARL)	• Preconditioning- ½ bed volume of 5% NaOH and 1% NaCN (½-1 hour) • 5 bed volumes hot water at 3 bed volumes per hour • 110°C • 50-100 kPa total cycle time 9 hours (including acid wash)	Advantages: • reduced reagent consumption • reduced carbon inventory • reduced size of stripping section Disadvantages: • use high temperatures and pressures • multiple streams increase circuit complexity
Alcohol Stripping	• 1% NaOH, 0.1% NaCN and 20% alcohol by volume (methanol) • 80°C • atmospheric pressure • 5-6 hours	Advantages: • reduced size of stripping section • less frequent carbon regeneration Disadvantages: • high fire risks associated with alcohol • high operating costs due to alcohol loss by volatilisation • number of safety features to minimise fire rises • effective vapour recovery system is essential to maintain economic balance
High Pressure Stripping	• 1% NaOH and 0.1% NaCN • 160°C • 350 kPa • 2-6 hours	Advantages: • reduced reagent consumption • reduced carbon inventory • reduced size of stripping section Disadvantages: • more costly equipment • effluent solution must be cooled before pressure reduction to avoid flashing

TABLE 1.1 The various types of elution processes available, along with their advantages and disadvantages.

Type of cell	Cell design	Operation of the cell
Cylindrical Cell	• Consists of three concentric cylinders which rest inside one another. The cathode compartment, the overflow container and the outside container • Cathode: The inner container is perforated and serves as the cathode. It contains a feed tube, a current distributor and a quantity of steel wool • Anode: The anode is contained in the outside container and is made up of stainless steel screen	Pregnant electrolyte enters through feed tube, and circulates upwar through the steel wool cathode. It the overflows into the outer container wi the anode made of stainless ste screen. The solution is the recirculated back to the elution section
Rectangular Cell	• Consists of a rectangular tank with the anodes and cathodes positioned alternately along length • Cathode: Consist of steel wool in rectangular plastic baskets. They are connected electrically in parallel by bus bars provided on the top of the cell on both sides. • Anodes: Consist of stainless steel sheets. They are connected the same as the cathodes	The pregnant solution is fed to one sid on the cell . It passes through the ce and overflows on the other side, wher it is recirculated to the elution section.
Anglo American Cell (AARL)	• Consists of a cylindrical annular design. The cell is divided into anode and cathode compartments by a cation permeable membrane. • Cathode: Consists of stainless steel wool in a sock shape. • Anode: The anode is stainless steel. A strong, alkaline solution in circulated through the anode compartment.	The electrolyte solution is circulate through the cathode compartment, afte which it is recirculated to the elutio section.

TABLE 1.2 The various types of electrowinning cells available.

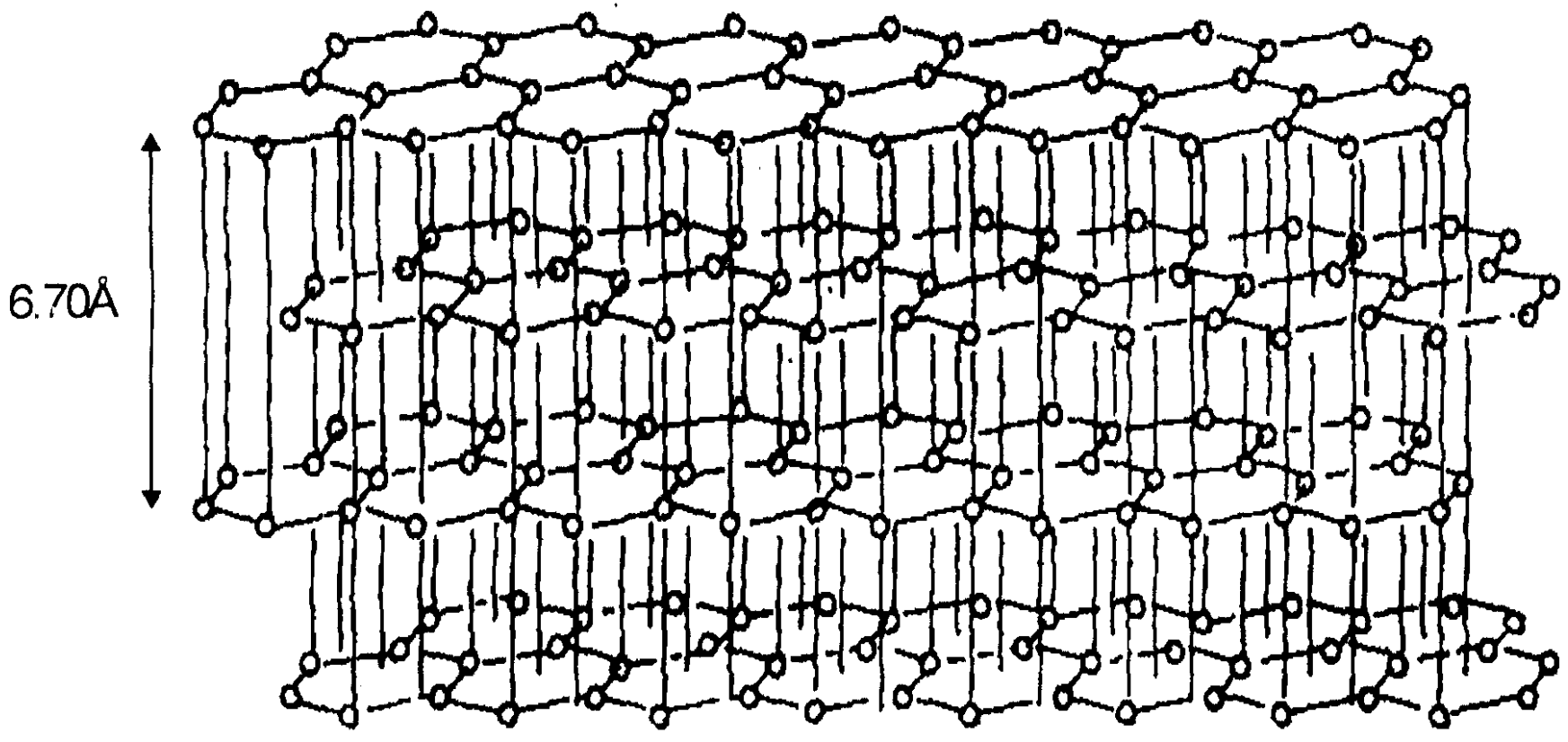

FIGURE 1.1 A schematic representation of the structure of graphite. The circles denote the position of carbon atoms, whereas the horizontal lines represent carbon-to-carbon bonds.

(After [*Bokros, 1969*])

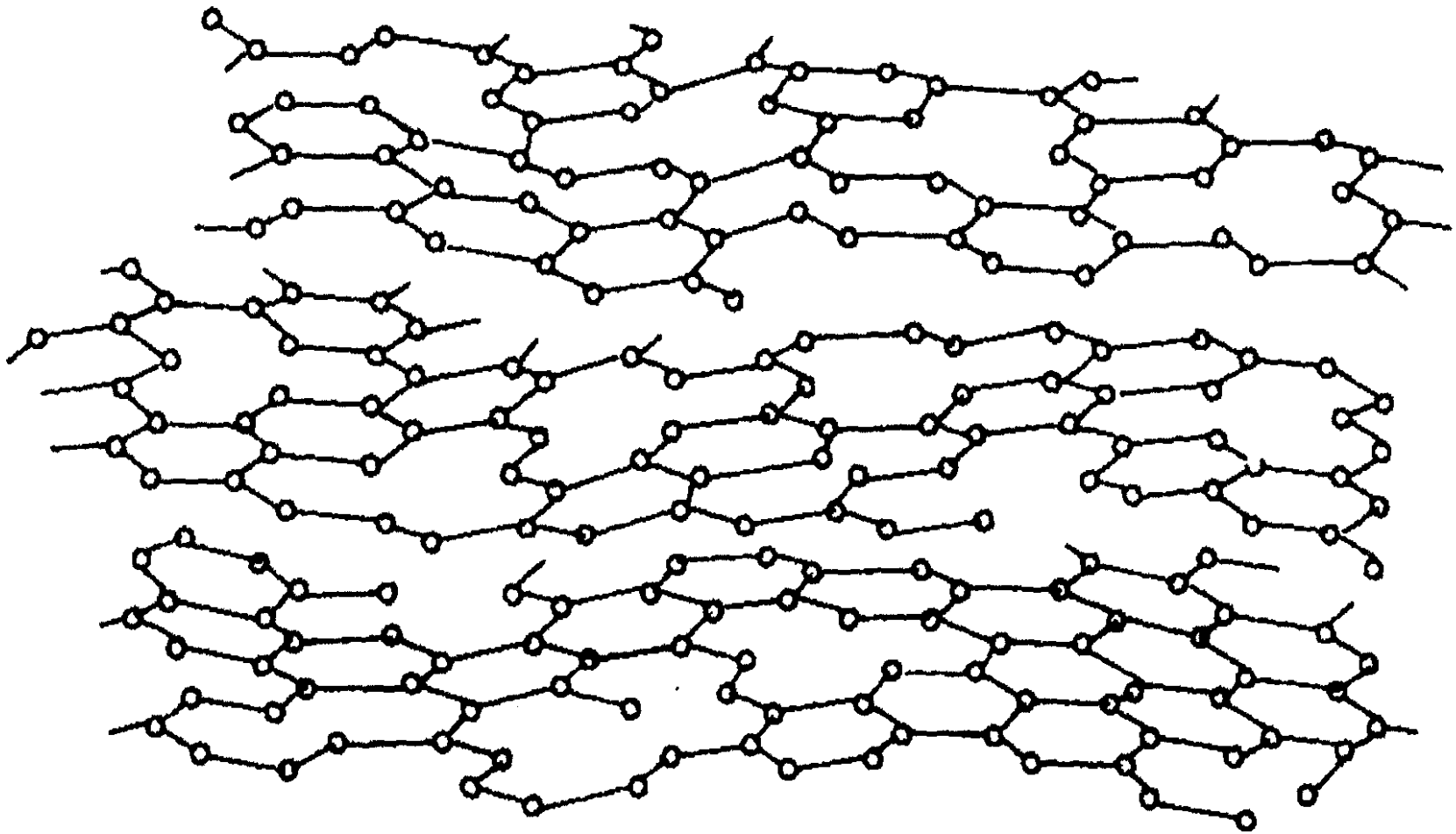

FIGURE 1.2 A schematic representation of the proposed structure of activated carbon. Oxygen-containing organic functional groups are located at the edges of broken graphite ring systems.
(After [*Bokros, 1969*])

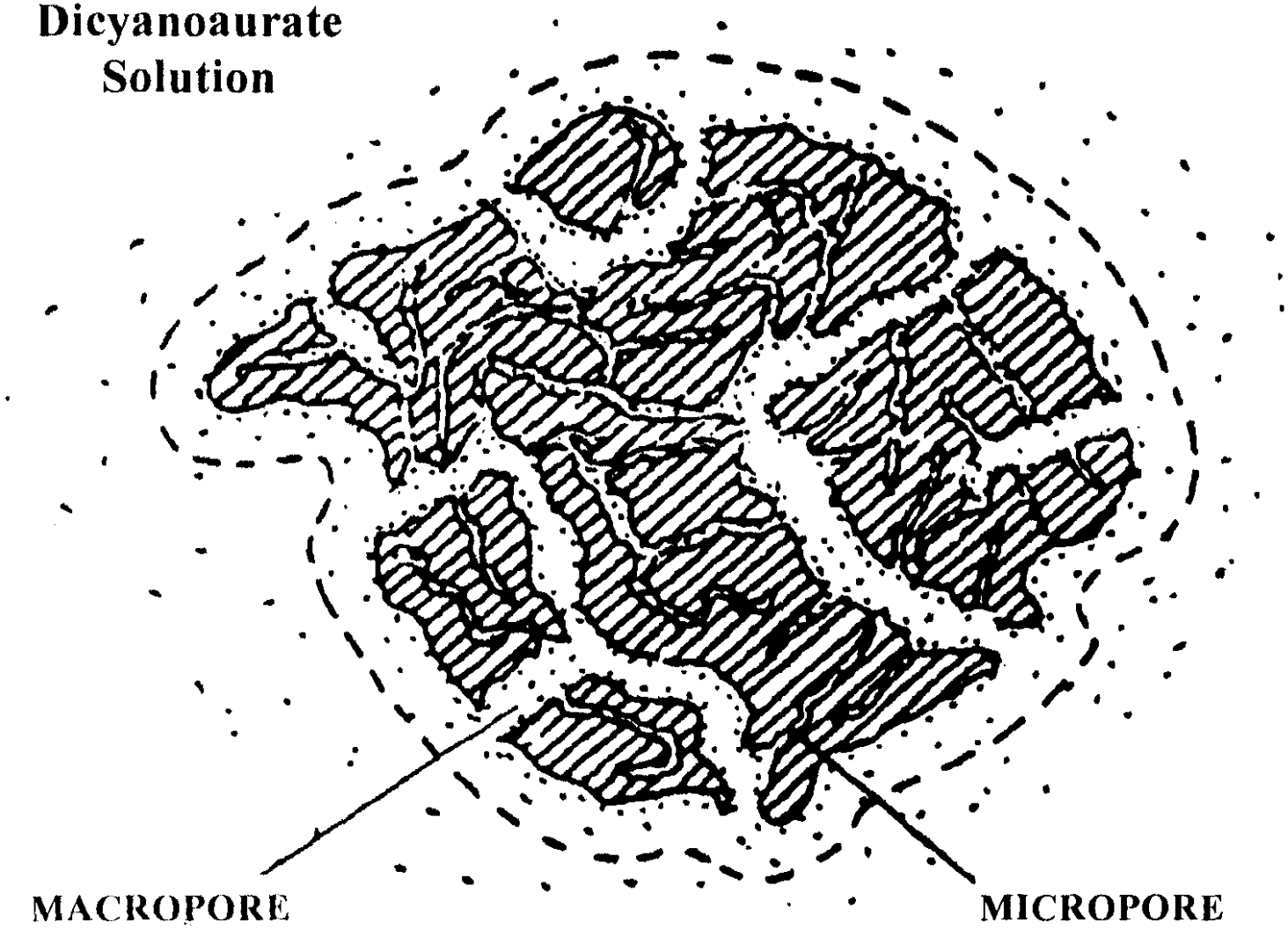

FIGURE 1.3 An illustration of the pore structure of activated carbon.
(After *[Bailey, 1987]*)

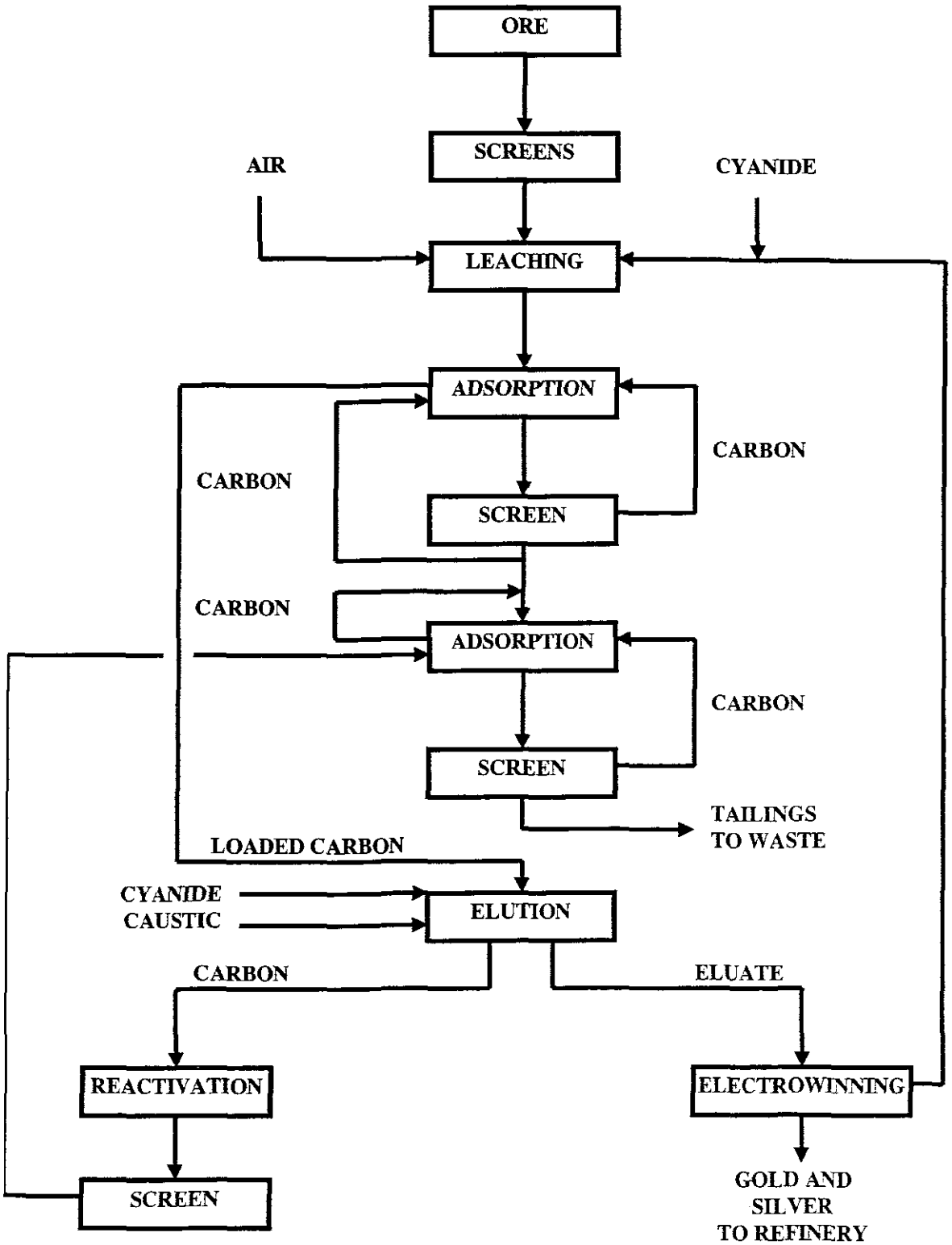

FIGURE 1.4 A flow diagram representing the Carbon-in-Pulp circuit.

CHAPTER 2

THEORY

This chapter deals with a model for gold adsorption onto activated carbon, which incorporates both external film diffusion and intraparticle diffusion. The model is by no means novel and has been used by numerous authors *[Liebenberg et al, 1997; van Deventer, 1986]*.

2.1 EQUILIBRIUM EXPRESSIONS

Equilibrium isotherms should have the following characteristics*[Weber et al, 1987]*:

- It should accurately describe the data for a particular system.
- It should be applicable for the widest possible range of equilibrium concentration values.
- It should, if possible, have some theoretical foundation.

There are three commonly used isotherms describing single solute adsorption from aqueous solutions, namely, the linear, Freundlich and Langmuir isotherms [Coulson et al, 1991].

2.1.1 Linear isotherm

$$Q_e = AC_e \tag{2.1}$$

Although this is one of the most widely used single solute isotherms, it is only applicable at very low adsorbate concentrations.

2.1.2 Freundlich isotherm:

$$Q_e = AC_e^{\,n} \tag{2.2}$$

This isotherm has one distinct disadvantage in that it does not approach true linearity at low equilibrium concentrations.

2.1.3 Langmuir Isotherm

$$Q_e = \frac{AC_e}{B + C_e} \tag{2.3}$$

At higher adsorbate concentrations the lack of space on the adsorbent hinders the adsorption process. Therefore the adsorption rate is proportional to the empty surface available on the adsorbent and also fluid concentration. At low absorbate concentrations the Langmuir isotherm is reduced to a linear form.

2.2 DIFFUSION MODEL: ASSUMPTIONS

The following assumptions apply to the diffusion model:

- The carbon particles are treated as perfect, uniform spheres,
- Isothermal conditions are assumed during adsorption,
- The adsorption reaction on the surface of the carbon occurs instantaneously,
- Local equilibrium exists at the solid-liquid interface,
- The macro- and micro-pores are homogeneously distributed throughout the carbon particle,
- The macro- and micropore's diameters are taken to be the weighted average diameter of all pores within the certain pore size range,
- The macro- and micropores are not interconnected, and both pore types extend from the particle surface to the centre of the particles.

2.3 MATERIAL BALANCE EQUATIONS

The Freundlich isotherm has often been used in the past to describe the equilibrium loading of the gold cyanide onto activated carbon.

$$q_s = AC_s^{\,n} \tag{2.4}$$

If film transfer determines the adsorption rate, diffusion through the liquid film surrounding the carbon particles can be described by Ficks's law:

$$n_L = k_f\left(C - C_s\right) \tag{2.5}$$

A mass balance over the batch stirring reactor yields:

$$-V\frac{dC}{dt} = n_L a_{carbon} \tag{2.6}$$

The carbon particles are assumed spherical so that:

$$a_{carbon} = \frac{6M}{d_p\rho} \tag{2.7}$$

Substituting equations 2.5 and 2.7 into 2.6 leads to:

$$-V\frac{dC}{dt} = \frac{n_L 6M}{d_p\rho} = \frac{k_f\left(C - C_s\right)6M}{d_p\rho} \tag{2.8}$$

Simplifying and substituting equation 2.4:

$$\frac{dC}{dt} = \frac{6k_f M}{d_p V \rho}\left[\left(\frac{q_s}{A}\right)^{\frac{1}{n}} - C\right] \tag{2.9}$$

From a mass balance over the reactor:

$$q_s = \frac{(C_i - C)V}{M} \tag{2.10}$$

Substituting equation 2.10 into equation 2.9 leads to:

$$\frac{dC}{dt} = \frac{6k_f M}{d_p V B \rho}\left(\frac{(C_i - C)V}{M}\right)^{\frac{1}{n}} - \frac{6k_f MC}{d_p V \rho} \tag{2.11}$$

where: $B = A^{\frac{1}{n}}$

The diffusion of solute into macro- and micropores can be described by equations (2.12) and (2.13) respectively:

$$\frac{dq_{macro}}{dt} = \frac{60D_{macro}}{d_p{}^2}\left(\frac{q_s{}^2 - q_{macro}{}^2}{2q_{macro}}\right) \tag{2.12}$$

$$\frac{dq_{micro}}{dt} = \frac{60D_{micro}}{d_p{}^2}\left(\frac{q_s{}^2 - q_{micro}{}^2}{2q_{micro}}\right) \tag{2.13}$$

The dimensions of equations (2.12) and (2.13) are kilograms per square meter of macropore area per second, and kilograms per square meter of micropore area per second respectively. However, the total area of the carbon particles is divided into a macropore-area kilogram carbon, A_{macro}, and a micropore-area per kilogram carbon, A_{micro}.

A mass balance at the external surface of the carbon yields the following equation:

$$\frac{6k_f M}{d_p \rho}(C - C_s) = \frac{60M}{d_p^{\,2}}\left[D_{macro} A_{macro}\right]\left[\frac{q_s^{\,2} - q_{macro}^{\,2}}{2q_{macro}}\right] + D_{micro} A_{micro}\left[\frac{q_s^{\,2} - q_{micro}^{\,2}}{2q_{micro}}\right] \tag{2.14}$$

2.4 PARAMETER ESTIMATION

2.4.1 External mass transfer coefficient

The liquid phase material balance in a batch reactor yields:

$$\frac{dC}{dt} = \frac{6k_f M}{d_p V \rho}(C_s - C) \tag{2.15}$$

Assumptions:

- the adsorption rate in the early stages of the batch process can be determined by film mass transfer, resulting in a linear concentration gradient form the bulk liquid to the adsorbent surface.
- the adsorbate concentration on the surface of the adsorbent (Cs) is negligibly small as compared to the adsorbate concentration in the bulk liquid.

If these two assumptions are made, equation 2.15 can be simplified to;

$$\frac{dC}{dt} = -\frac{6k_f M}{d_p V \rho} C \tag{2.16}$$

Integrating equation 2.16 yields:

$$\ln\left(\frac{C_o}{C}\right) = \frac{6k_f M}{d_p V \rho} t \qquad t \to 0 \tag{2.17}$$

An expression for k_f is then found:

$$k_f = \frac{\ln\left(\frac{C_o}{C}\right)}{t} \frac{d_p V \rho}{6M} \tag{2.18}$$

To determine the value of k_f experimentally, $\ln(C_o/C)$ vs time is plotted for the initial stages of the adsorption process.

2.4.2 Intraparticle diffusivity

The surface diffusion coefficient, D, in the homogeneous surface diffusion model is actually a lumped intraparticle diffusion coefficient. These parameters can be estimated by using the Runga-Kutta solution for the batch kinetics of a single solute in a Powell least squares regression routine *[van Deventer, 1984]*.

CHAPTER 3

EXPERIMENTAL

This chapter describes the experimental procedures and analytical techniques which were used to conduct the work contained in this thesis.

3.1 EXPERIMENTAL MATERIAL

A pyrite ore, supplied by Hartebeesfontein gold mine, was used in this study. The ore was firstly ground and screened to obtain the required particle size distribution of 80% under 75 μm and 20% between 106 and 75 μm. Pyrite ores are refractory in nature and contain encapsulated gold particles. It was therefore necessary to leach the ore using $CaCN_2$ to remove any gold which might have been released during grinding. After leaching, the ore was washed using distilled water and dried overnight in an oven at 50 °C.

Coconut shell activated carbon, supplied by Norit and National Chemical Products Ltd in South Africa, was used in the study. The virgin carbon was first washed with distilled water to remove any fines. The washed carbon was dried overnight in an oven at 50 °C and was then stored in an airtight Schutt-bottle to avoid adsorption of moisture from the atmosphere.

All reagents used in experimental work were of analytical grade, and distilled water was used throughout. The absorbate used in all experiments was potassium dicyanoaurate, $KAu(CN)_2$, a crystalline salt of 98% purity. A mass of 1.493 g of the $KAu(CN)_2$ was weighed off and made up in a 1 L volumetric flask using distilled water, the product being a standard solution of

1000 ppm Au in the form $Au(CN)_2^-$. This solution was in turn diluted in 1 L volumetric flasks to produce the various concentrations required for the experimental work.

Laboratory grade Calcium Hydroxide, $Ca(OH)_2$, was used to adjust the pH to the required level, and the ionic strength was kept constant in all experiments.

3.2 EXPERIMENTAL SET-UP

The experiments described in sections 3.3 - 3.5 were performed in 1 L perspex reactors. These reactors were made to a standard tank configuration, with an internal diameter of 110 mm and a height of 150 mm. They were fitted with 4 evenly spaced baffles each with a width of 10 mm. The agitation was provided by a 3-blade impeller with a diameter of 45 mm, driven by a Heidolph electric motor. A sketch of the apparatus is shown in Figure 3.1.

3.3 MINIMUM STIRRING SPEEDS

Test were performed to determine the minimum stirring speeds required to keep slurries of various densities in suspension. The effect of stirring inefficiencies on particle distribution were also investigated. The ore to water ratio in these experiments were as follows:

1100 $kg.m^{-3}$:	160 g ore	: 940 g water
1300 $kg.m^{-3}$:	475 g ore	: 825 g water
1500 $kg.m^{-3}$:	795 g ore	: 705 g water
1600 $kg.m^{-3}$:	950 g ore	: 650 g water

The reactors were mounted on a frame over a mirror so that the bottom of the tank could be observed. A high initial stirring speed was used to ensure all solids were in suspension, the stirring speed was then reduced until settling was observed.

3.4 EQUILIBRIUM ISOTHERM

A carbon concentration of 0.5 $g.l^{-1}$ was used with gold concentrations in the range of 5 - 30 ppm. The stirring speed was kept constant at 300 rpm to ensure that all the carbon was kept in suspension. As these experiments were run over 72 hours, the reactors fitted with perspex lids to prevent spillage or evaporation of samples. The pH was kept constant at 11.

3.5 BATCH EXPERIMENTS

These experiments were performed to determine the effect of changes in slurry density, carbon concentration, gold concentration and stirring speed on the adsorption kinetics of gold onto activated carbon. Carbon concentrations of 1 - 3 $g.l^{-1}$ were used for each variation in slurry density, gold concentration and stirring speed.

3.6 ANALYTICAL METHODS

A varian Techtron AA-1275 atomic adsorption spectrophotometer (AA) with an air-acetylene flame was used to determine the concentration of gold in solution.

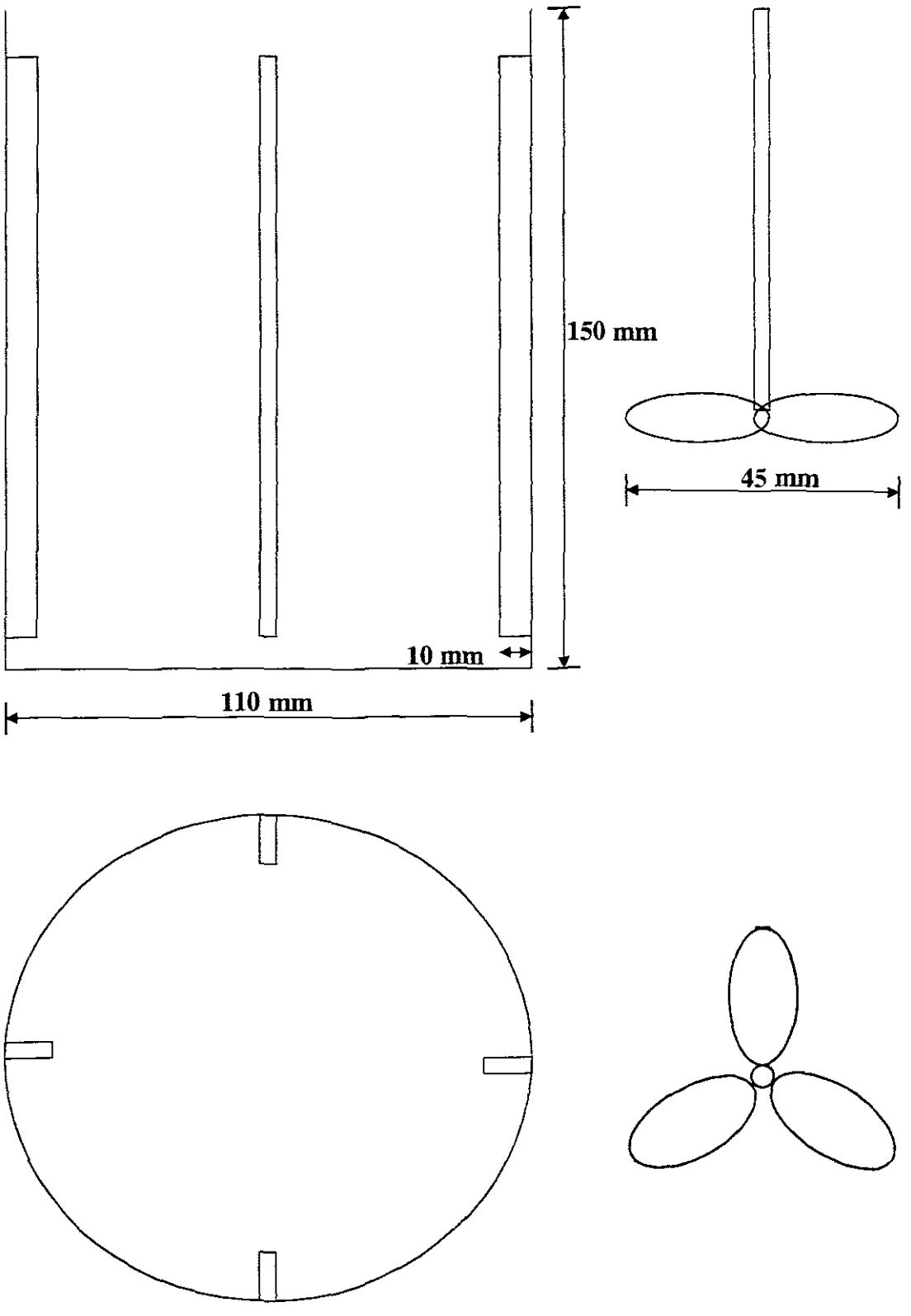

FIGURE 3.1 The apparatus for experiments performed in 1 L reactors

CHAPTER 4

EQUILIBRIUM ISOTHERM

This chapter explains the equilibrium isotherm for the adsorption of aurocyanide onto activated carbon. An accurate estimation of the equilibrium conditions is essential when modelling CIP plants. This ensures effective adsorption in each stage, by avoiding equilibrium conditions being attained. Furthermore, all derivations contained in this work cannot be used once equilibrium conditions have been attained.

4.1 EQUILIBRIUM EXPERIMENTS

The experimental procedure for equilibrium determination is described in Chapter 3, section 3.4. The following results were obtained:

Q_e ($mg.g^{-1}$)	C_e ($mg.l^{-1}$)
6.844	1.732
16.448	2.396
22.578	4.490
25.146	6.985
31.772	14.195

Linear regression was used to fit the experimental data to the three types of isotherms discussed in Chapter 2. The three expressions are:

Linear Isotherm $$Q_e = 2.791C_e \quad (4.1)$$

Freundlich Isotherm $$Q_e = 7.072C_e^{0.565} \quad (4.2)$$

Langmuir Isotherm $$Q_e = \frac{161.29Q_e}{32.839 + C_e} \quad (4.3)$$

The linearisation procedure for the three isotherms is illustrated in Figures 4.1 - 4.3. It was found that the Freundlich isotherm best explained the equilibrium loading of gold onto activated carbon. This is graphically illustrated in Figure 4.4.

Further proof that the Freundlich isotherm provides the best fit can be seen from the R^2 values which describe the goodness of fit of the predicted Qe values to the experimental Qe values.

Linear - $R^2 = 0.853$

Freundlich - $R^2 = 0.934$

Langmuir - $R^2 = 0.911$

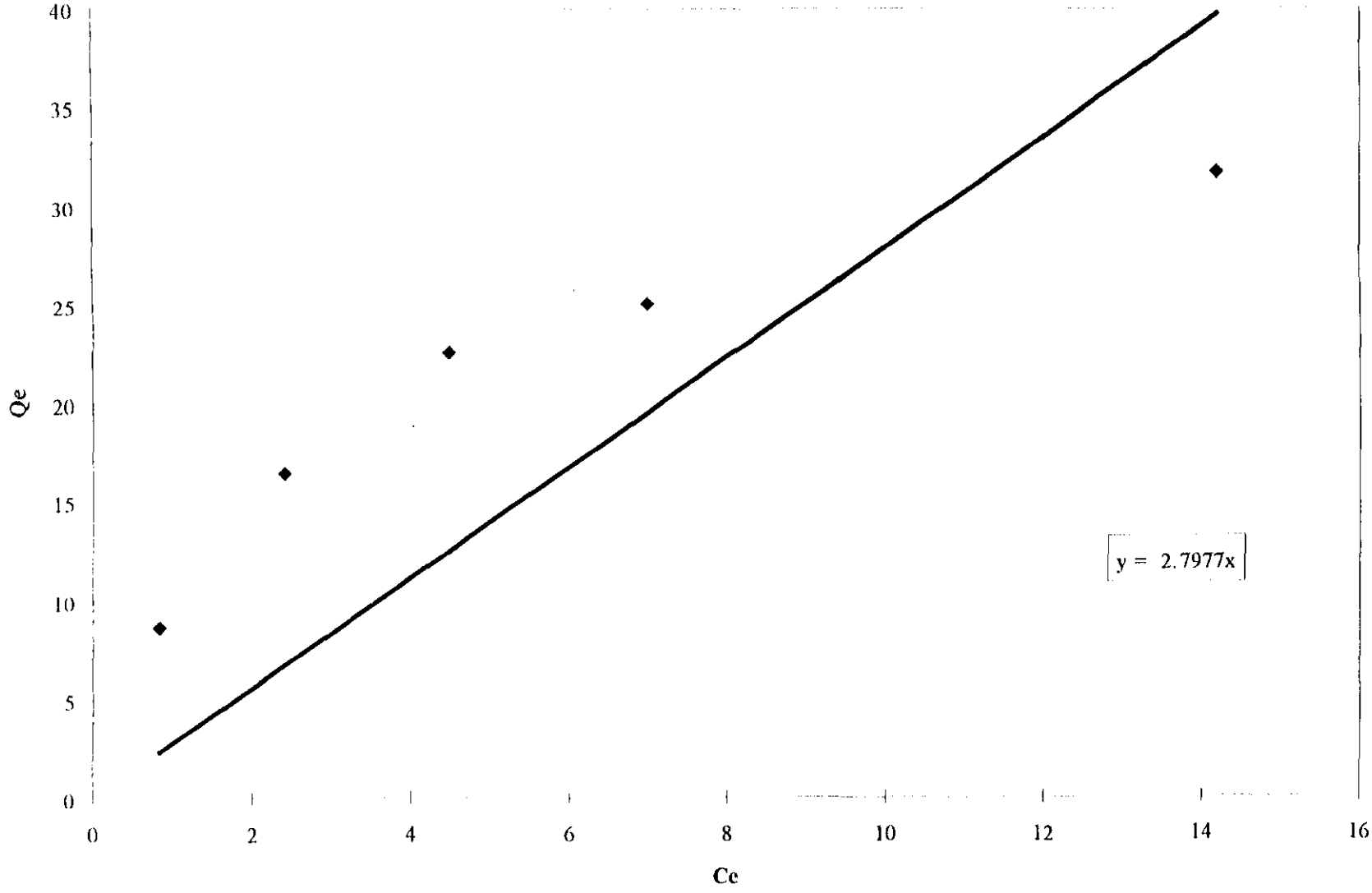

FIGURE 4.1 **A graphical representation of the linear form of the Linear isotherm.**

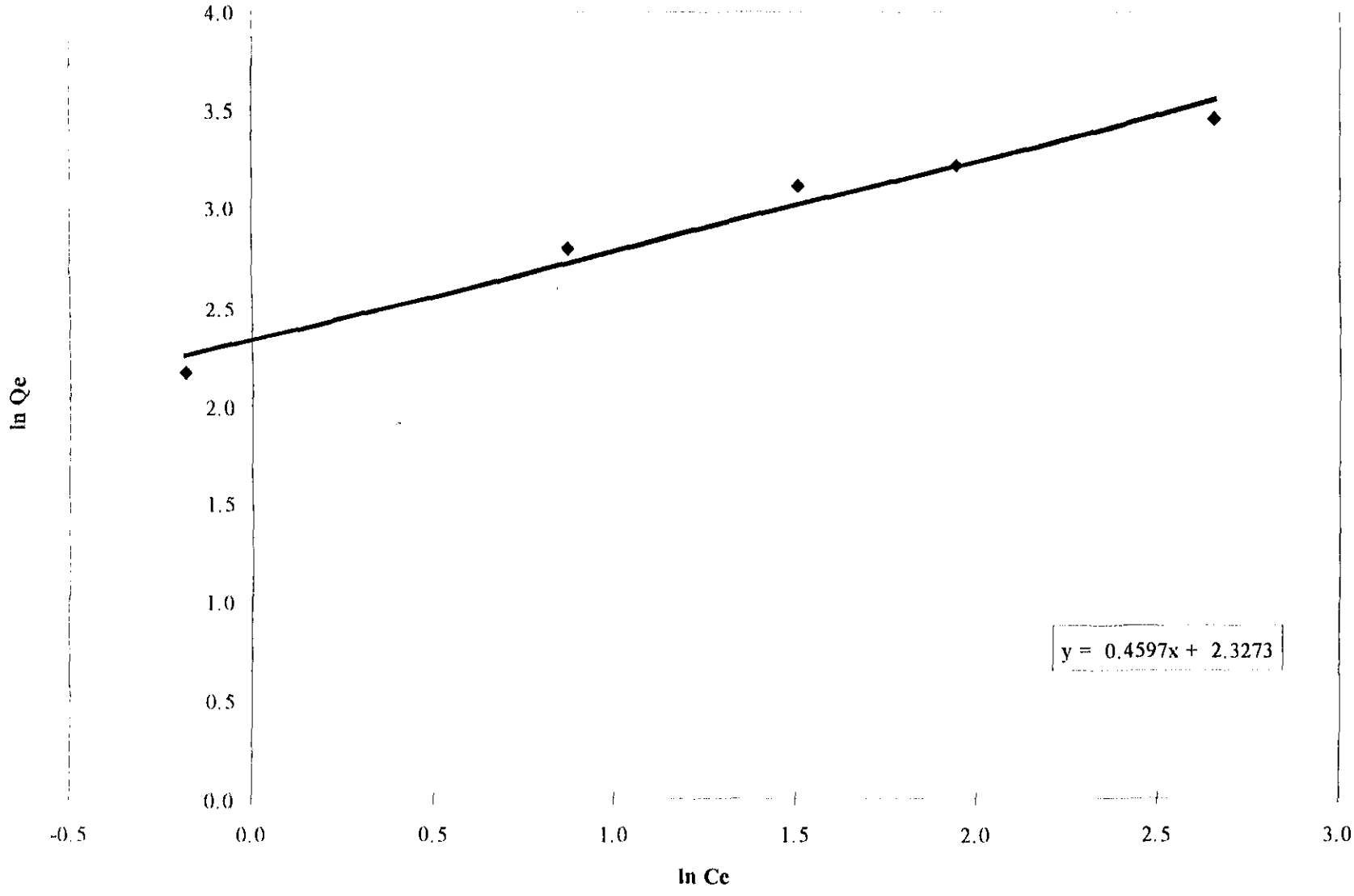

FIGURE 4.2 **A graphical representation of the linear form of the Freundlich isotherm**

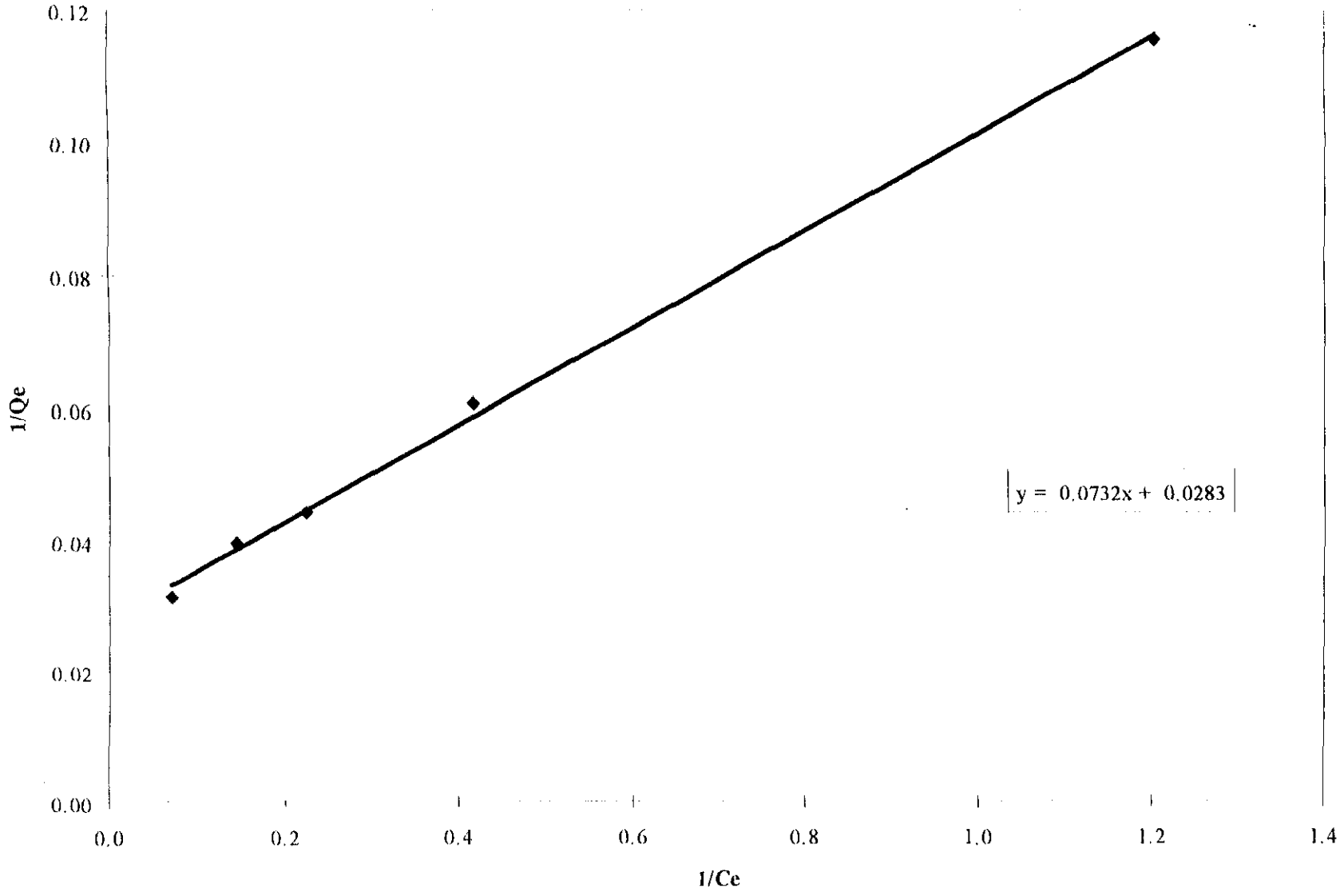

FIGURE 4.3 **A graphical representation of the linear form of the Langmuir isotherm.**

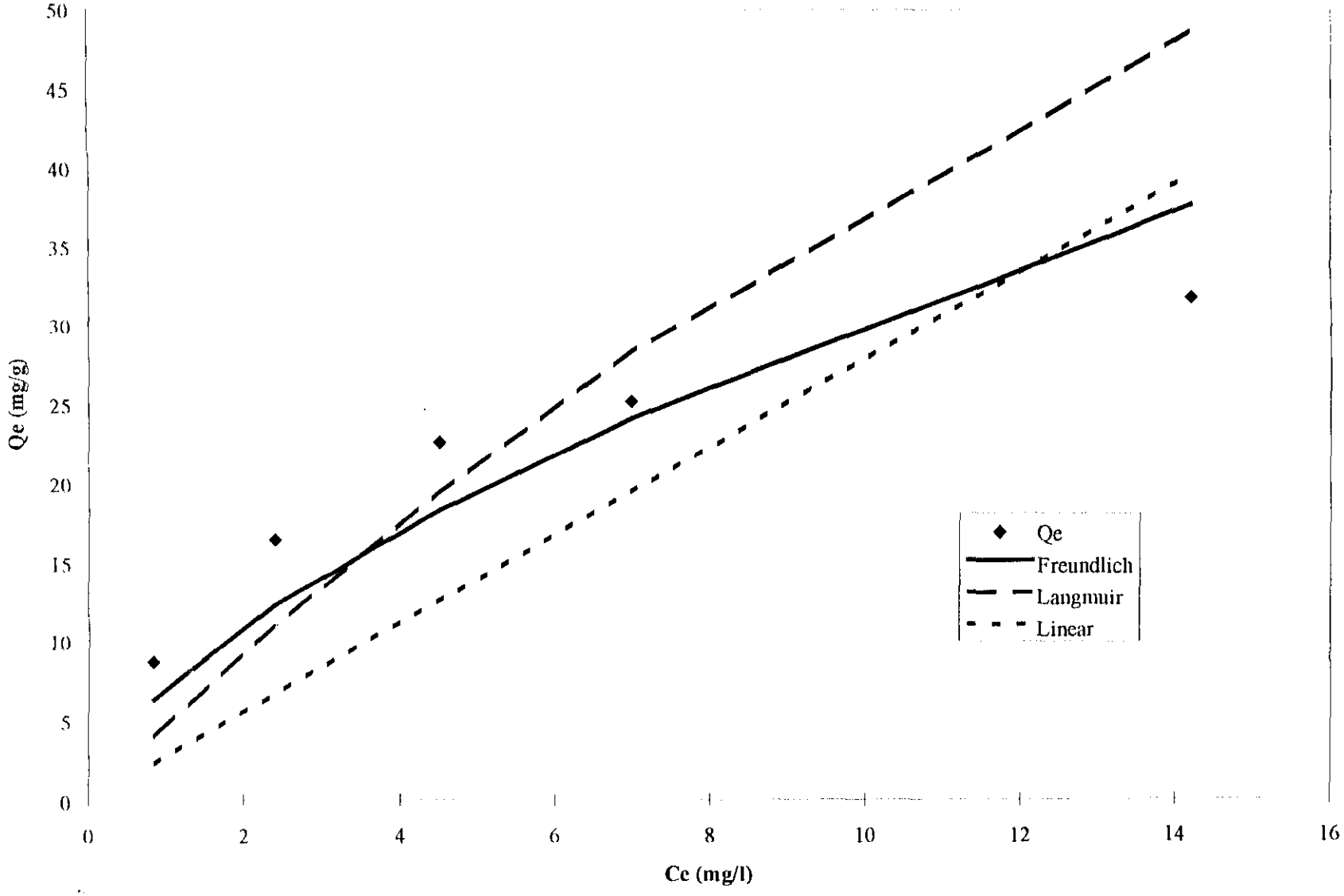

FIGURE 4.4 **A graphical representation showing how the predicted Qe values of the Freundlich , Langmuir and Linear isotherms fit the experimental data**

CHAPTER 5

THE EFFECT OF DENSITY AND STIRRING SPEED ON THE EXTERNAL MASS TRANSFER COEFFICIENT

During gold adsorption onto activated carbon, the constant rate period is controlled mainly by film diffusion with negligible intraparticle diffusion. *[Mathews et al, 1976].*

In this chapter the effect of slurry density and agitation rate on the external mass transfer coefficient (k_f) is investigated. The equation for k_f was derived in Chapter 2 as:

$$k_f = \frac{\ln\left(\frac{C_o}{C}\right)}{t} \cdot \frac{d_p V \rho}{6M} \qquad (5.1)$$

Batch experimental data was used to determine the effects of density and stirring speed on the various k_f values. Additional information used for the calculations included:

- carbon density of 750 $kg.m^{-3}$
- average carbon diameter of 0.0015 m

5.1 THE EFFECT OF SLURRY DENSITY

Slurry densities of 1100, 1300 and 1500 $kg.m^{-3}$ were used, with a constant stirring speed of 520 rpm and carbon concentration of 1 $g.l^{-1}$. The k_f values for these experiments are shown in Table 5.1. and is graphically illustrated in Figure 5.1.

From Figure 5.1 it can be seen that there is a general increase in the external mass transfer coefficient with an increase in slurry density. The slurry density has two effects on the mass transfer:

- the increased number of particles present in the solution result in more eddies being formed, which in turn improves the mixing efficiency of the system.
- the increased number of particles present also increase the occurrence of "blinding" of the carbon surface. This inhibits the dicyanoaurate from reaching the carbon surface.

The increase in external mass transfer with higher slurry densities show that the effects caused by the increased mixing efficiency outweighs the effects of increased blinding at a stirring speed of 520 rpm with the Reynolds number for mixing being 9.782×10^5.

5.2 THE EFFECT OF STIRRING SPEED

A slurry density of 1300 $kg.m^{-3}$ was used in this section, with stirring speeds of 450, 520, and 590 rpm. The results are shown in Table 5.2 and graphically illustrated in Figure 5.2. There are two effects stirring speed could have on the diffusion of gold through the film layer:

- An increased stirring speed results in a decrease in film thickness, as can be seen by the following relationship:

$$k_f = \frac{D}{x_f} \qquad (5.2)$$

Thus, film thickness is inversely proportional to k_f.

- The increased movement of the slurry particles due to increased agitation can increase the "blinding" phenomenon present, thereby reducing mass transfer through the film boundary.

From the results it can be seen that the increase in stirring speed initially has a negative effect on k_f. This can be explained by the larger role played by increased blinding, which out-weighs the effect of increased mixing. However, with a further increase in stirring speed there is an increase in k_f. This shows that the effect of the improved mixing becomes progressively larger than the "blinding" effect. Thus, it can be said that the combined effects of slurry density and agitation rate is by no means a simple one. This issue is further discussed in the next chapter.

5.3 THE EFFECTS OF GOLD AND CARBON CONCENTRATIONS

An increase in gold or carbon concentration will increase the external mass transfer coefficient and therefore the adsorption rate. This can directly be observed by the modification of Equation 5.1 to:

$$k_f = \frac{\ln\left(\frac{C_o}{C}\right)}{t} \cdot \frac{d_p \rho}{6} \cdot \frac{1}{C_c} \qquad (5.3)$$

where: Cc is the carbon concentration ($g.l^{-1}$)

$\frac{\ln\left(\frac{C_o}{C}\right)}{t}$ is the slope of a plot of the initial gold concentration divided by the concentration at time t (t^{-1})

5.4 SUMMARY

- An increase in slurry density increases the mass transfer coefficient at a Reynolds number of 9.782×10^5.
- An increased stirring speed initially decreases the mass transfer coefficient. However, further increases in stirring speed results in an increase in the mass transfer coefficient. This is due to the progressively increased effect of mixing over the negative blinding effect.

Slurry density ($kg.m^{-3}$)	Initial gold concentration (ppm)	k_f ($m.s^{-1}$)
1100	10	0.00176
	7	0.00153
	5	0.00158
1300	10`	0.00167
	7	0.00171
	5	0.00191
1500	10	0.00180
	7	0.00244
	5	0.00205

TABLE 5.1 k_f values for densities 1100, 1300 and 1500 $kg.m^{-3}$ at a constant stirring speed of 520 rpm.

(Experiments 19, 22, 25, 37, 40, 43, 55, 58 and 61)

Stirring Speed (rpm)	Intial gold concentration (ppm)	k_f ($m.s^{-1}$)
450	10	0.00233
	7	0.00215
	5	0.00215
520	10	0.00167
	7	0.00171
	5	0.00191
590	10	0.00230
	7	0.00207
	5	0.00203

TABLE 5.2 k_f values for stirring speeds of 450, 520 and 590 rpm at a constant density of 1300 $kg.m^{-3}$.

(Experiments 28, 31, 34, 37, 40, 43, 46, 49 and 52)

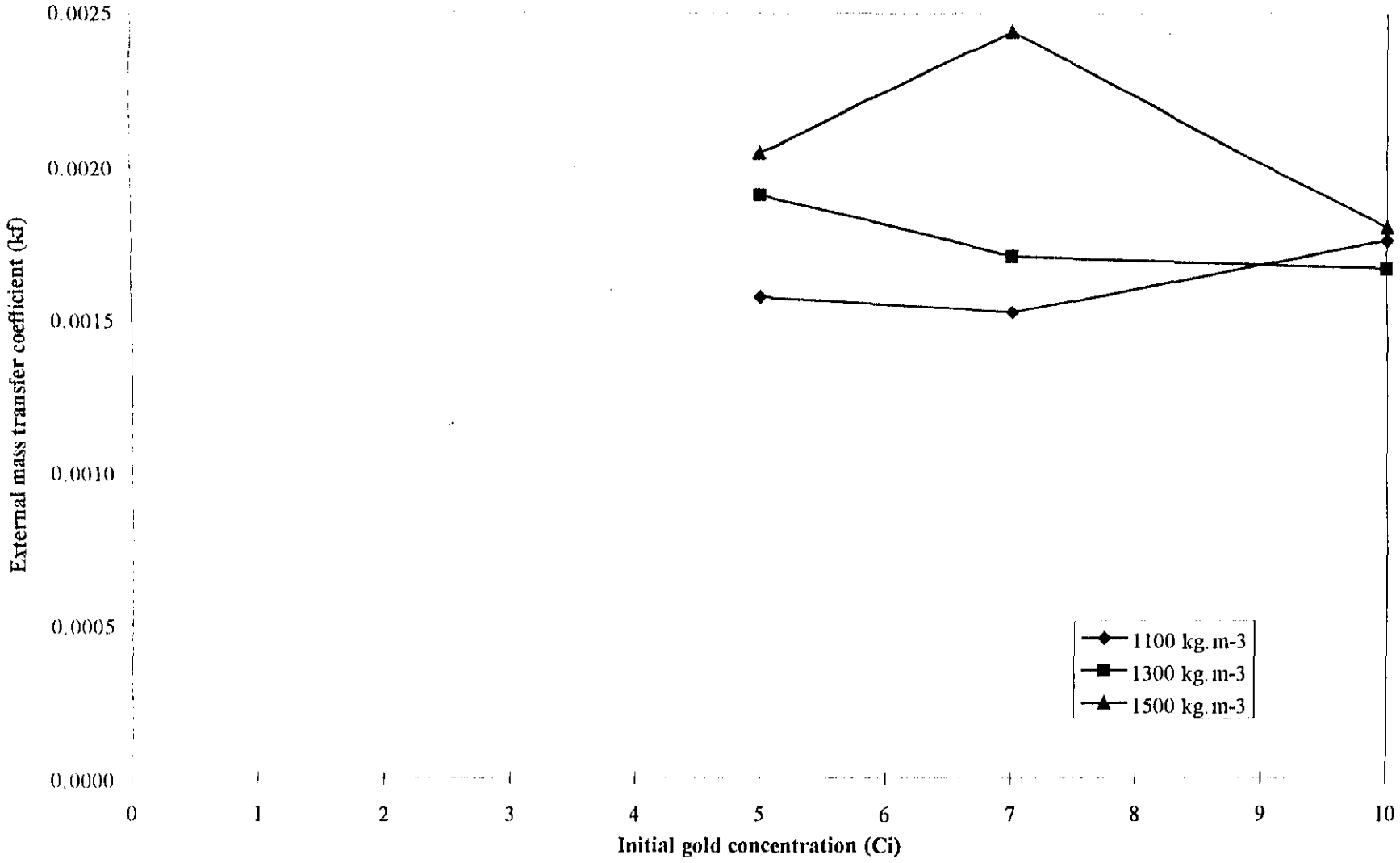

FIGURE 5.1 **A graphical representation of the k_f values for densities 1100, 1300 and 1500 kg.m^{-3} at a constant stirring speed of 520 rpm.**

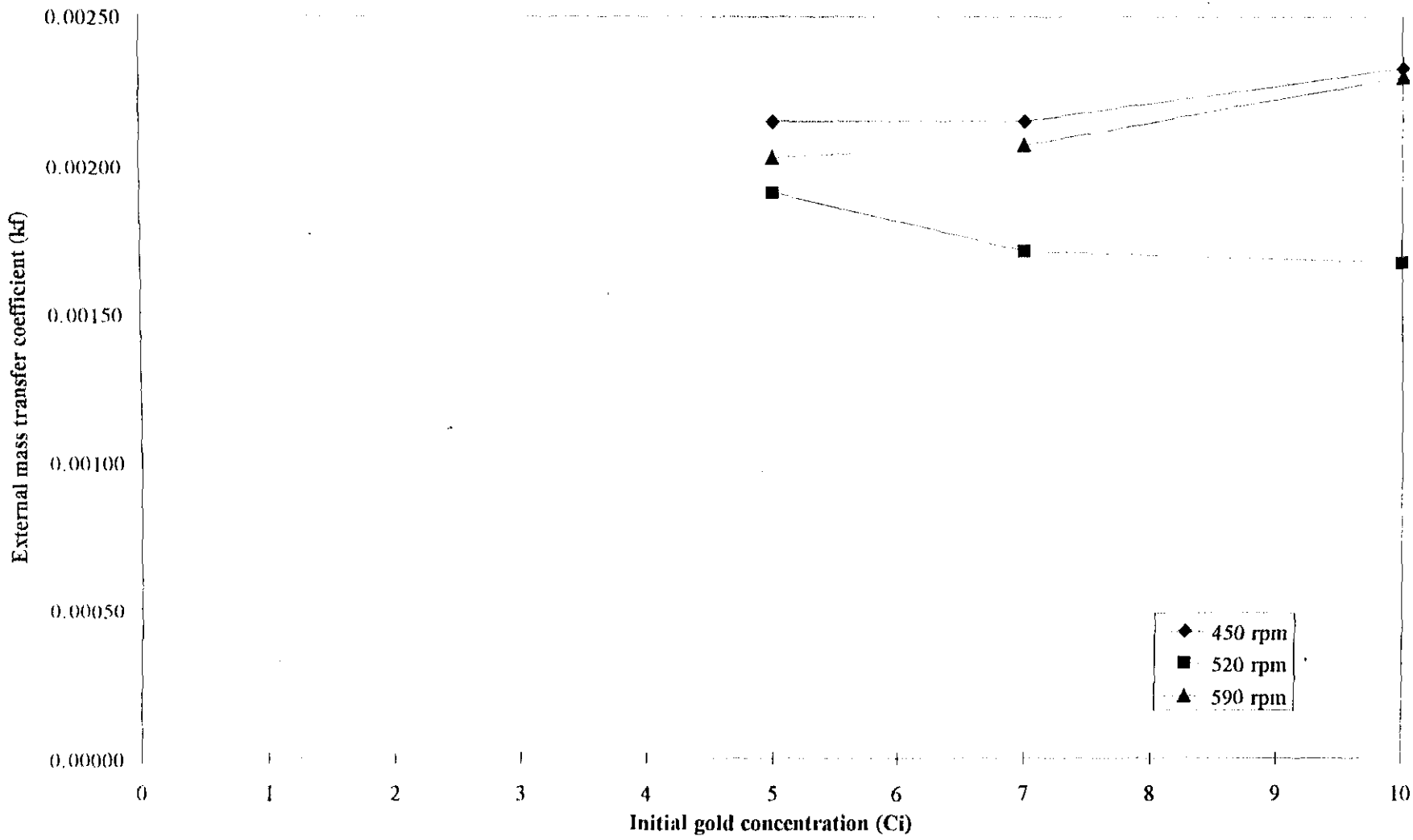

FIGURE 5.2 **A graphical representation of the k_f values for stirring speeds of 450, 520 and 590 rpm at a constant density of 1300 kg.m^{-3}.**

CHAPTER 6

THE EFFECTS OF SOLUTION CONCENTRATION, CARBON LOADING, SLURRY DENSITY AND STIRRING SPEED ON ADSORPTION KINETICS

The adsorption of gold cyanide onto activated carbon takes place in two stages:

- diffusion through the boundary film layer
- adsorption into the carbon pores

Film diffusion is controlled by the concentration gradient which exists across the film boundary layer. Thus, solution concentration and carbon loading are two of the main factors affecting adsorption rate. This chapter deals with the effect of these two parameters, along with the effects of slurry density, stirring speed and carbon concentration on the adsorption kinetics of gold cyanide onto activated carbon.

Much literature is available on the effects of various parameters on the adsorption process *[Bailey, 1987; Jones et al, 1989; McDougall, 1980; Petersen et al, 1993]*. However, these investigators view the process as a whole. Thus, an attempt was made to evaluate the effects of these parameters individually and to derive expressions incorporating their combined effects on the process.

6.1 THE GOLD ADSORPTION PROFILE

When investigating the effects of any parameter on the adsorption process, it becomes apparent that the magnitude of their effects vary along the adsorption profile. Upon investigation it became apparent that the adsorption profile in a batch reactor can be divided into two sections, namely:

- the constant rate period
- the diminishing rate period

This is graphically illustrated in Figure 6.1.

In practice, most plants attempt to operate in the constant rate period, so as to maximise the adsorption rate. Therefore, it was important to identify the point at which the constant rate period ends and the diminishing rate period commences in order to maintain an efficient process. It has been found that the initial gold concentration, agitation rate, slurry density and carbon concentration influence adsorption kinetics in the constant rate period. This was expected since all the above mentioned parameters will have an effect on film transfer which is the rate controlling factor in the initial stages.

During the diminishing rate adsorption period only carbon concentration and loading and solution concentration influenced the kinetics significantly. External adsorbent effects such as agitation rate and slurry density had a negligible effect. This phenomenon manifested the belief that intraparticle diffusion becomes the rate controlling factor in the diminishing rate period and cannot be influenced by additional mass transfer through the film boundary.

The "turning point" was mainly influenced by the initial solution concentration, slurry density, stirring speed and carbon concentration. However, it was found that initial gold concentration was the only significant effect.

The magnitude of the different effects is discussed in later sections in this Chapter.

6.2 SLURRY DENSITY AND STIRRING SPEED VERSUS POWER CONSUMPTION

Slurry density and stirring speed will have an effect on the power consumption of the circuit. Power consumption is an important consideration when attempting to optimise a circuit, for the purpose of profit maximisation.

The minimum agitation rate for complete suspension of the solid particles for each slurry density was determined by visual inspection. The relationship between minimum agitation rate and slurry density is exponential, as can be seen in Figure 6.2, and can be expressed as follows:

$$N_{min} = 0.023\rho^{0.81}$$

It should also be noted that a linear relationship exists between the power number and Reynolds number for this mixing system. This linear relationship is graphically illustrated in Figure 6.3.

6.3 CONSTANT RATE PERIOD

Linear regression techniques were applied to evaluate the effects of the parameters listed in section 6.2 on adsorption kinetics. After analysing the results obtained from experiments it became apparent that the effect of slurry density and agitation rate was not a simple one. Solid particles blind the carbon surface resulting in decreased mass transfer. However, changes in slurry density also have an effect on the mixing process. Similarly, agitation rate has a twofold effect. Firstly, increased stirring increases the turbulence in the system. However, this increased mixing also results in additional blinding of the carbon surface. A combined effect was thus found and mixing and blinding terms identified:

$N^{1.1}.RD$ - mixing

$N.RD^3$ - blinding

Where: N - agitation rate (rpm)

RD - relative density ($kg.m^{-3}$)

The relationship describing adsorption kinetics is shown in Table 6.1. The goodness of fit of these equations to the actual experimental data can be seen in Table 6.2.

Furthermore, it can be seen in Figure 6.4 that the adsorption rate at 520 rpm, given the tank configuration specified in Figure 3.1, is highest at density 1300 $kg.m^{-3}$.

6.4 TURNING POINT

Although carbon loading has an insignificant effect during constant rate adsorption, a point is reached where it can no longer be ignored. This point is determined mainly by the initial solution concentration. The results can be seen in Table 6.2, and show that higher initial solution concentrations result in increased solution concentrations at the turning points.

6.5 DIMINISHING RATE PERIOD

The carbon loading has a negligible effect on the constant rate period. However, this is not the case for the diminishing rate period. It is during this section of adsorption that the effect of the carbon loading becomes more pronounced. The rate of intraparticle diffusion is the rate controlling factor. In other words, the rate of gold transfer from the surface of the adsorbent to the inner structure of the pores becomes the limiting factor. Hence, it is not expected that the external factors such as mixing and blinding will have any significant effect on the process.

The results of the linear regression procedure are shown in Table 6.5, with the R^2 values both with and without mixing and blinding. As can be seen from this table mixing and blinding have a very small effect on the adsorption rate. These results therefore showed that:

- no external factors have significant effects on the adsorption rate.
- no additional pore blockage occurs as a result of the increase in the number of particles in solution or increase in agitation rate.

The relationship between solution concentration and carbon loading which describes its effect on adsorption rate is:

$$S^{1.1}/C_L^{0.5}$$

From this relationship it can be seen that the solution concentration has a positive effect on the adsorption rate, while carbon loading has a negative effect. Furthermore, it can be seen from the slopes that a percentage increase in solution concentration will have a far greater effect than the same percentage increase in carbon loading. This effect is illustrated in Figure 6.5.

6.7 SUMMARY

- The gold adsorption profile can be divided into two sections: constant rate period and a diminishing rate period.
- The two main factors which affect gold adsorption are solution concentration and carbon loading.
- Slurry density and stirring speed affect the external factors of mixing ($N^{1.1}.RD$) and "blinding" ($N.RD^3$).
- The following exponential relationship exists between the minimum stirring speed and agitation rate:

$$N = 0.023\rho^{0.81}$$

- A linear relationship exists between Reynolds number and power number.
- Adsorption during the constant rate period is controlled mainly by film diffusion. The carbon loading has a negligible effect on the adsorption rate, which accounts for the constant adsorption rate. Mixing and "blinding" also play a significant role in the adsorption rate during this period.
- The turning point, or point at which constant rate ends and the diminishing rate period begins, is controlled mainly by the initial solution concentration.
- The final adsorption rate is controlled mainly by intraparticle diffusion, with only solution concentration and carbon loading having a significant effect on the process.

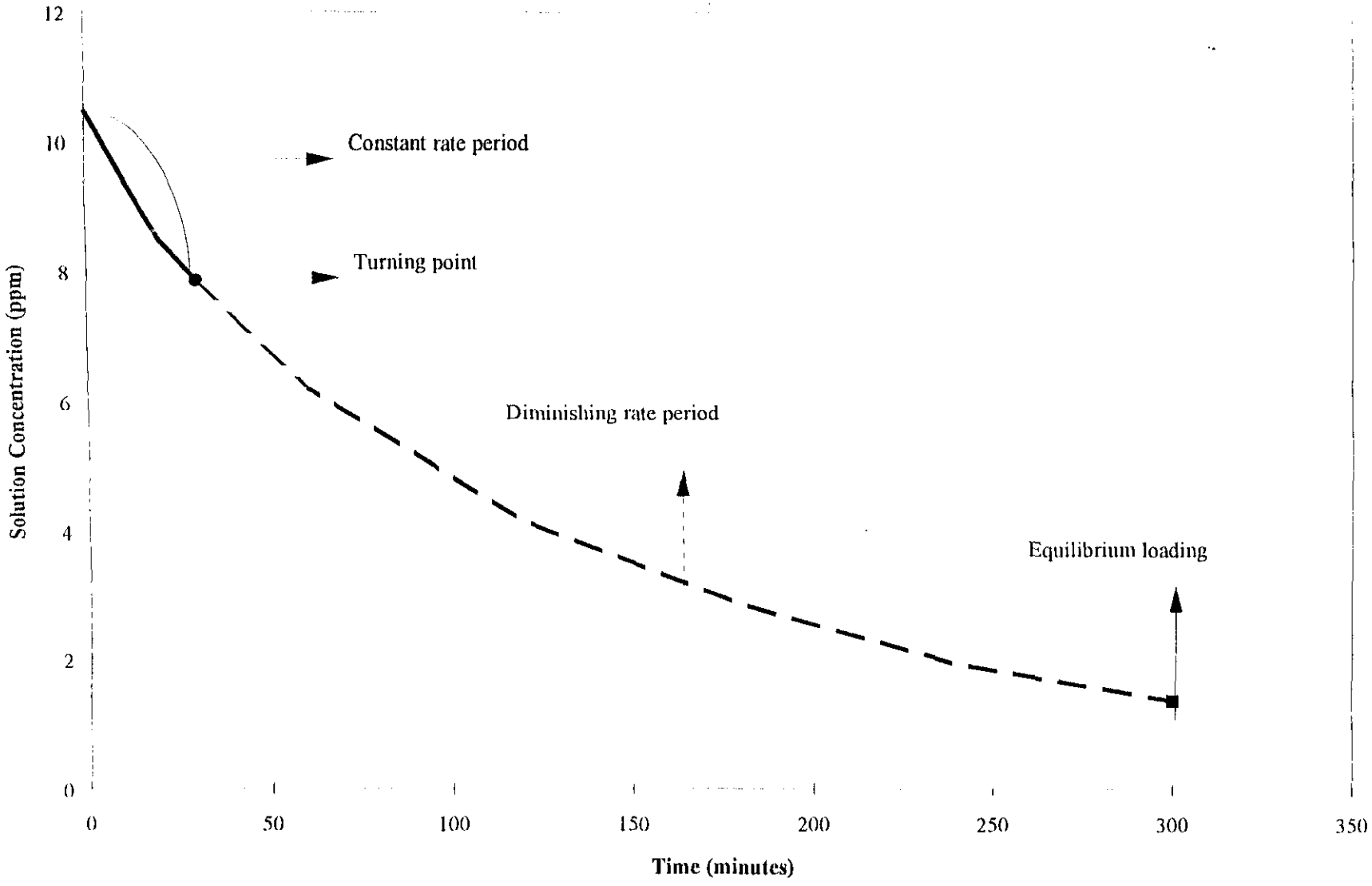

FIGURE 6.1 The various sections of an gold adsorption profile.

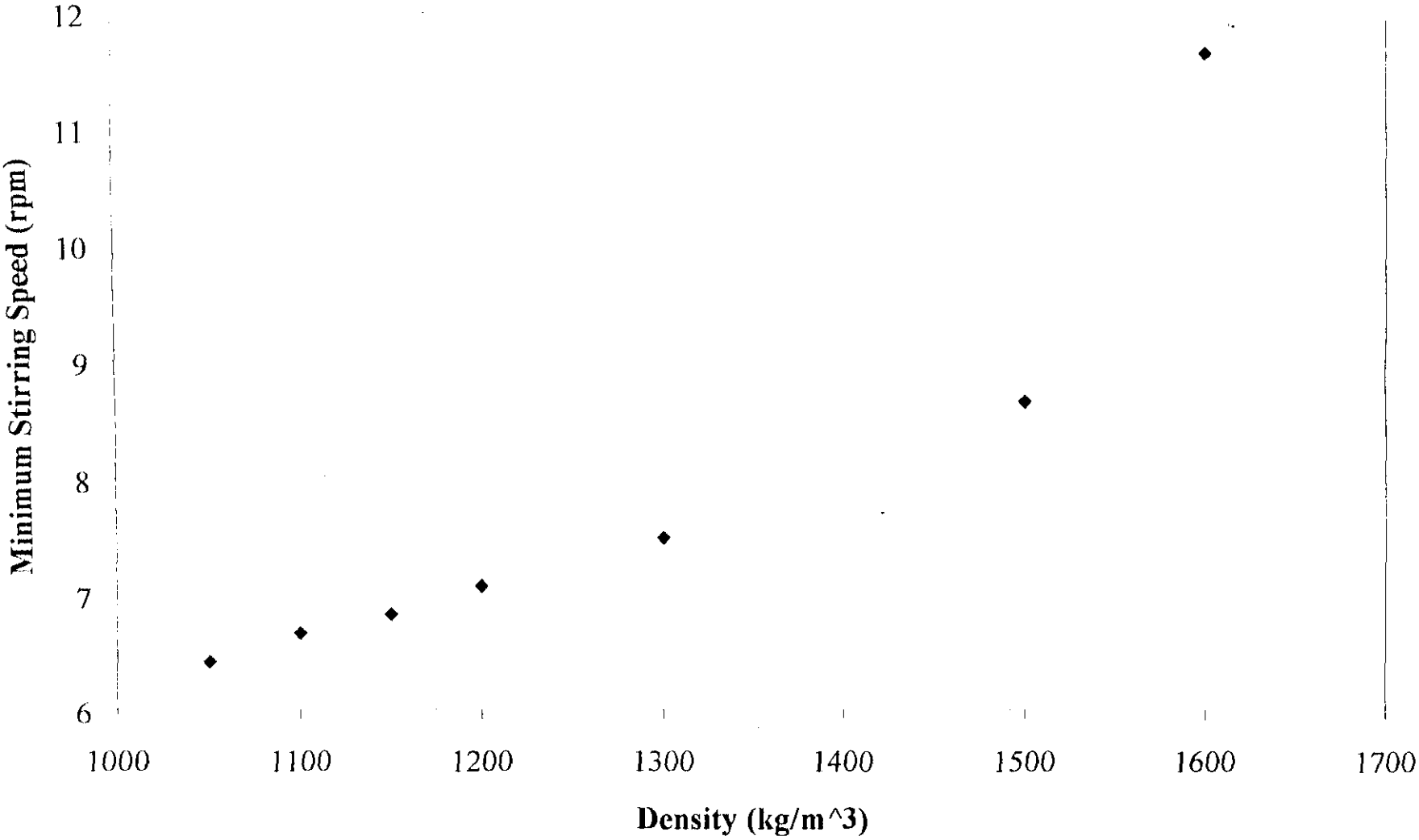

FIGURE 6.2 A graphical representation of the exponential relationship between minimum stirring speed and slurry density.

(See Appendix A)

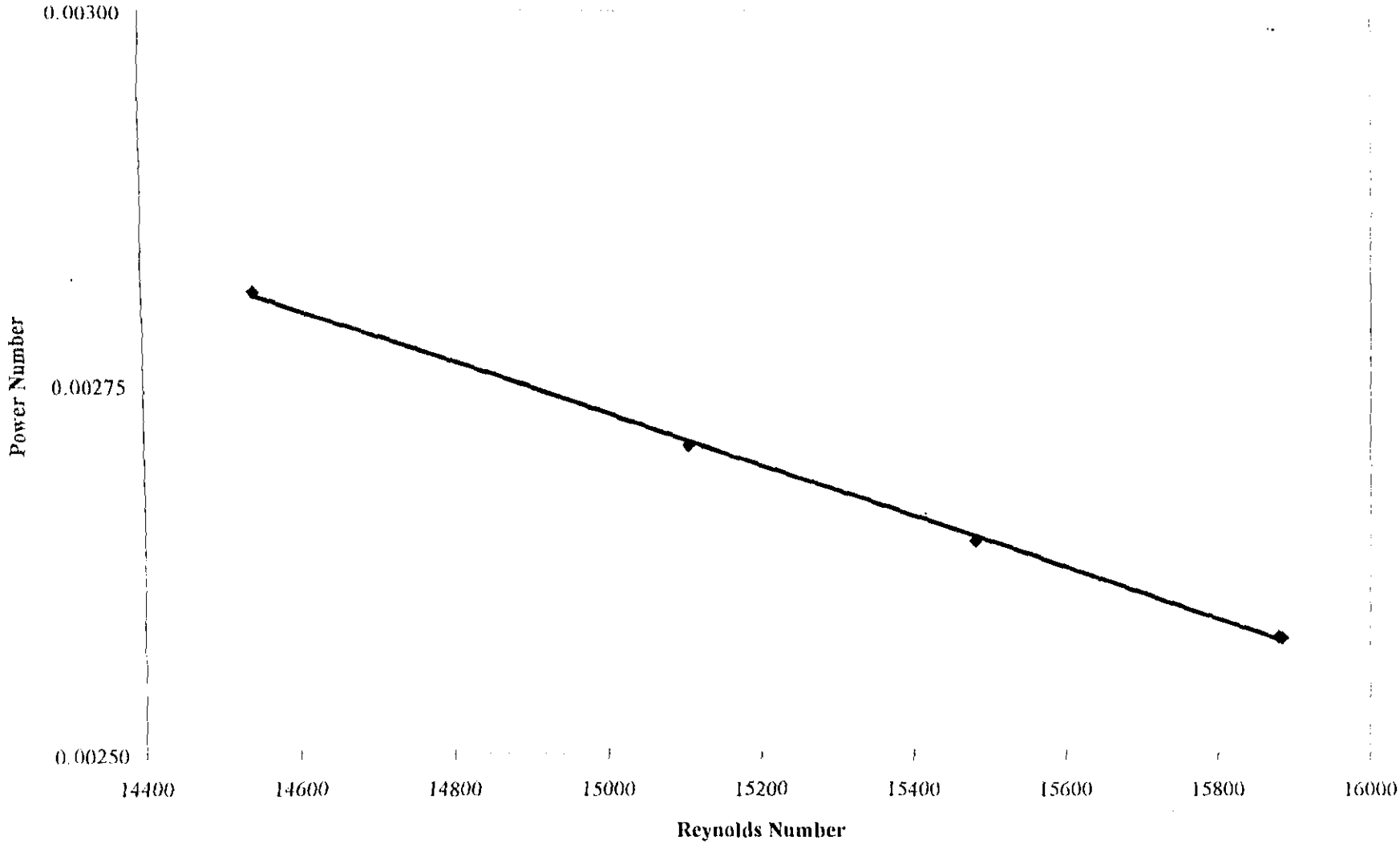

***FIGURE 6.3* A graphical representation of Reynolds number versus power number.**

(See Appendix A)

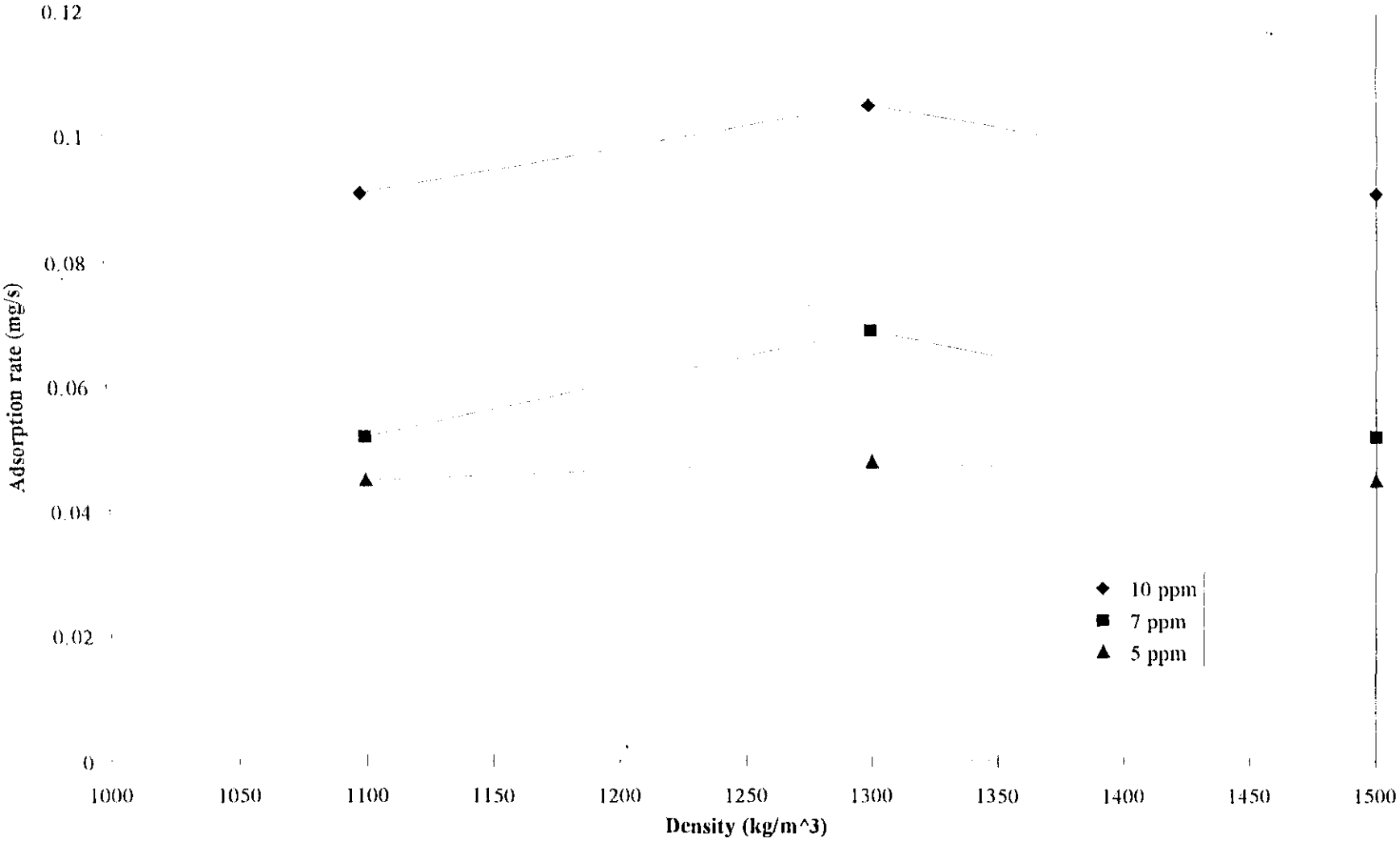

FIGURE 6.4 The effects of changing density on the gold adsorption rate during the constant rate period at a stirring speed of 520 rpm.

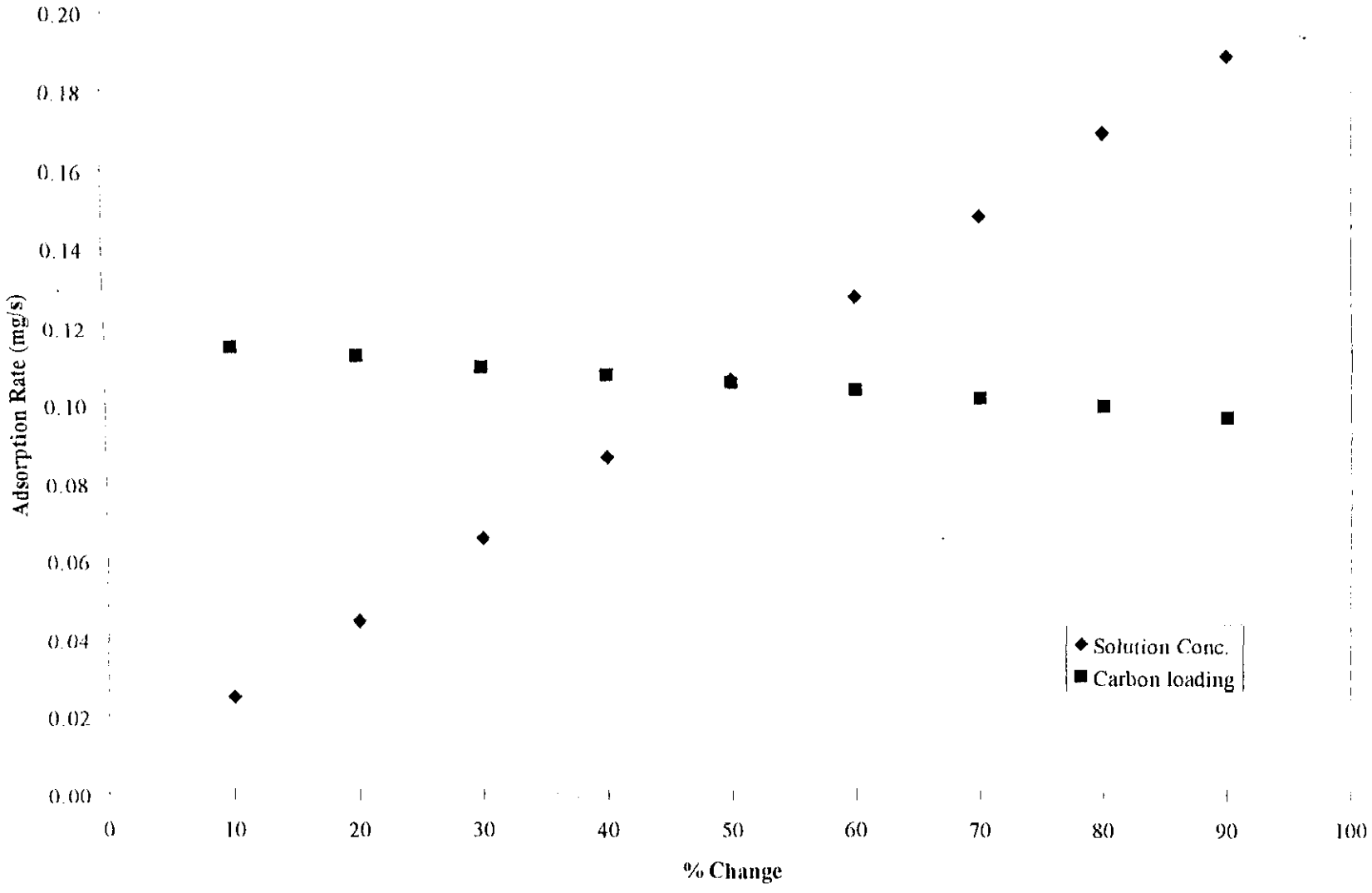

FIGURE 6.5 The effects of changes in solution concentration and carbon loading on the gold adsorption rate.

Carbon concentration ($g.l^{-1}$)	Slurry density ($kg.m^{-3}$)	Equation	R^2
1	1100	$R = +0.600 + 0.008C_i + 0.540M - 0.607B$	0.943
	1300	$R = +1.240 + 0.009C_i + 0.873M - 0.707B$	0.987
	1500	$R = -0.018 + 0.027C_i + 0.010M - 0.002B$	0.766
2	1100	$R = +2.981 + 0.015C_i + 3.201M - 3.533B$	0.943
	1300	$R = 0.117 + 0.022C_i + 0.004M - 0.008B$	0.983
	1500	$R = +1.153 + 0.044C_i + 0.550M - 0.341B$	0.941
3	1100	$R = -0.075 + 0.010C_i + 0.005M - 0.0004B$	0.969
	1300	$R = +11.45 + 0.040C_i + 8.493M - 6.842B$	0.950
	1500	$R = -0.211 + 0.032C_i + 0.063M - 0.025B$	0.991

TABLE 6.1 The effects of initial solution concentration, slurry density and stirring speed on the constant rate period.

Stirring speed (rpm)	Initial solution concentration ($mg.l^{-1}$)	Actual adsorption rate ($mg.s^{-1}$)	Predicted adsorption rate ($mg.s^{-1}$)
400	10	0.091	0.085
	7	0.052	0.060
	5	0.045	0.043
460	10	0.069	0.073
	7	0.055	0.052
	5	0.035	0.034
520	10	0.071	0.070
	7	0.048	0.050
	5	0.034	0.033

TABLE 6.2 The goodness of fit of the predicted values to the experimental data during the constant rate period. Carbon concentration of 1 $g.l^{-1}$ and slurry density of 1100 $kg.m^{-3}$.

The standard error, or standard deviation of the predicted values from the actual experimental data is 0.0056.

Carbon concentration ($g.l^{-1}$)	Equation	R^2
1	$TP = -0.448 + 0.763C_i$	0.880
2	$TP = -0.442 + 0.578C_i$	0.904
3	$TP = -0.996 + 0.682C_i$	0.841

TABLE 6.3 The effects of initial solution concentration, slurry density and stirring speed on the turning point.

Stirring speed (rpm)	Initial solution concentration ($mg.l^{-1}$)	Actual solution concentration at "turning point" ($mg.l^{-1}$)	Predicted solution concentration at "turning point" ($mg.l^{-1}$)
400	10	8.267	7.436
	7	5.722	5.047
	5	3.670	3.368
460	10	7.861	7.519
	7	5.540	5.364
	5	3.200	3.587
520	10	7.642	7.256
	7	5.909	5.346
	5	4.047	3.603

TABLE 6.4 The goodness of fit of the predicted values to the experimental data for the "turning point". Carbon concentration of 1 $g.l^{-1}$ and slurry density of 1100 $kg.m^{-3}$.

The standard error, or standard deviation of the predicted values from the actual experimental data is 0.619.

Carbon concentration ($g.l^{-1}$)	Slurry density ($kg.m^{-3}$)	Equation	R^2 (excluding mixing and blinding)	R^2 (including mixing and blinding)
1	1100	$R = 0.0039 + 0.0099\, S^{1.1} / C_l^{0.5}$	0.875	0.889
	1300	$R = 0.0032 + 0.0110\, S^{1.1} / C_l^{0.5}$	0.876	0.877
	1500	$R = 0.0021 + 0.0102\, S^{1.1} / C_l^{0.5}$	0.882	0.888
2	1100	$R = 0.0026 + 0.0366\, S^{1.1} / C_l^{0.5}$	0.937	0.945
	1300	$R = 0.0036 + 0.0348\, S^{1.1} / C_l^{0.5}$	0.846	0.900
	1500	$R = 0.0019 + 0.0306\, S^{1.1} / C_l^{0.5}$	0.896	0.906
3	1100	$R = 0.0045 + 0.0550\, S^{1.1} / C_l^{0.5}$	0.852	0.863
	1300	$R = 0.0091 + 0.0562\, S^{1.1} / C_l^{0.5}$	0.854	0.868
	1500	$R = 0.0057 + 0.0284\, S^{1.1} / C_l^{0.5}$	0.837	0.860

TABLE 6.5 The effects of solution concentration, carbon loading slurry density and stirring speed on the diminishing rate period.

Slurry density ($kg.m^{-3}$)	Stirring speed (rpm)	Time (minutes)	Actual adsorption rate ($mg.s^{-1}$)	Predicted adsorption rate ($mg.s^{-1}$)
1100	400	60	0.045	0.037
		180	0.017	0.011
		300	0.007	0.007
1300	450	60	0.021	0.033
		180	0.013	0.010
		300	0.005	0.057
1500	520	60	0.030	0.038
		180	0.017	0.017
		300	0.010	0.010

TABLE 6.6 The goodness of fit of the predicted values to the experimental for the diminishing rate period. Carbon concentration of 1 $g.l^{-1}$ and intial solution concentration of 10 $mg.l^{-1}$.

The standard error, or standard deviation of the predicted values from the actual experimental data with densities: 1100 $kg.m^{-3}$ = 0.0045

1300 $kg.m^{-3}$ = 0.0045

1500 $kg.m^{-3}$ = 0.0025

CHAPTER 7

CONCLUSIONS

The aim of this study was to investigate the combined effects of operating parameters such as pulp density, agitation rate, gold concentration and carbon concentration, on the adsorption of aurocyanide onto activated carbon.

- The equilibrium isotherm conditions for the coconut shell activated carbon is well explained by the following Freundlich type isotherm :

$$Q_e = 7.325 C_e^{0.565}$$

This condition serves as a guideline in using the adsorption rate predictions, as these predictions are no longer valid once equilibrium has been reached.

- It was shown that an increase in agitation rate does not necessarily increase adsorption rate. This is the effect of a complex interaction between slurry particles and fluid motion.

- A mixing ($N^{1.1}.RD$) and a blinding ($N.RD^3$) number was developed using linear regression techniques to explain the complex interaction between fluid motion and solid particles in suspension.

- OLS estimation proved to be effective in predicting the adsorption of aurocyanide onto activated carbon.

- The constant rate adsorption was found to be linear and of the following form:

  $$\text{Rate} = \text{Constant}_1 + \text{Constant}_2(\text{Ci}) + \text{Constant}_3(\text{M}) - \text{Constant}_4(\text{B})$$

  Also, constant rate adsorption is a function of gold concentration, carbon concentration, agitation rate and slurry density.

- The point at which constant rate adsorption is replaced by a diminishing rate of adsorption was found to be a strong function of solution concentration:

  $$\text{TP} = \text{Constant}_1 + \text{Constant}_2(\text{Co})$$

- The diminshing rate of adsorption was found to be a function of solution concentration, carbon loading and carbon concentration:

  $$\text{Rate} = \text{Constant}_1 + \text{Constant}_2(S^{1.1}/CL^{0.5})$$

  This result confirmed that intraparticle diffusion is the rate controlling factor during this stage with "external" particle effects such as slurry density and agitation rate not influencing the rate.

- All the above findings are based on adsorption in a standard tank batch configuration. Further work will be required to test the accuracy of the relationships derived in a continuous process with different tank configurations.

CHAPTER 8

FUTURE WORK

The work performed in this study provides the bases for further work that will include:

- The construction of a laboratory scale pilot plant capable of operating on a counter-current or co- counter-current bases. This plant will be used to investigate the effects of the two modes of operation on parameters such as:
  - carbon abrasion
  - backmixing

  It will also be used to determine if the effects predicted by batch experiments could be used to predict the effects experienced during plant conditions.
- The eventual incorporation of all the experimental data to formulate a computer package which will assist plant operators in the optimisation of the carbon-in-pulp circuit. Figure 8.1 shows a flow diagram of the proposed computer program.

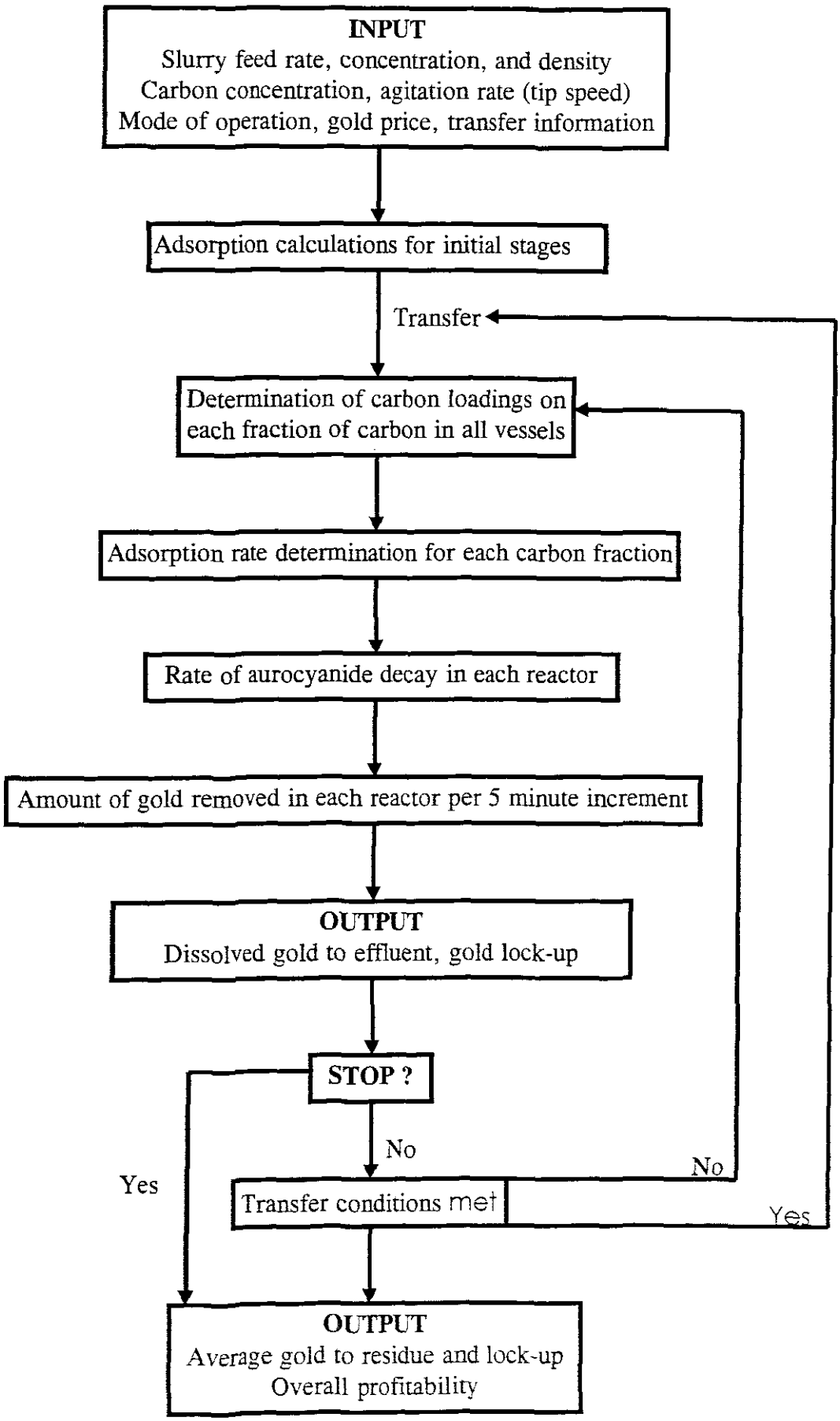

FIGURE 8.1 **A flow diagram of the proposed computer package.**

NOMENCLATURE

a_{carbon}	external surface area of carbon	m^2
A	parameter in Freundlich isotherm	
A_{macro}	total macro pore area	m^2
A_{micro}	total micro pore area	m^2
B	parameter in isotherm	
C	Solute concentration (mass fraction)	$mg.l^{-1}$
C_e	Equilibrium solution concentration	$mg.l^{-1}$
C_i	Initial solution concentration	$mg.l^{-1}$
C_o	oxygen concentration	$mg.l^{-1}$
C_s	solution concentration at liquid-adsorbent interface	$mg.l^{-1}$
d_p	diameter of adsorbent particles	m
D	Diffusion coefficient	$m^2.s^{-1}$
D_{macro}	diameter of macropores	m
D_{micro}	diameter of micropores	m
J	Membrane permeation rate	$m.s^{-1}$
k_f	external film transfer coefficient	$m.s^{-1}$
M	mass of adsorbent	kg
N	agitation rate	rpm
N_{min}	minimum agitation rate	rpm
n	exponent in Freundlich isotherm	
n_L	rate of diffusion through liquid film	$mg.m^{-2}.s^{-1}$
q_{macro}	solute loading into macropores	$mg.g^{-1}$
q_{micro}	solute loading into micropores	$mg.g^{-1}$
q_s	solute loading at solution-adsorbent interface	$mg.g^{-1}$
Q_e	equilibrium loading onto adsorbent	$mg.g^{-1}$

R	rate of adsorption	$mg.s^{-1}$
R_g	Universal gas constant (8.314)	$J.kmol^{-1}.K^{-1}$
t	time variable	s
T	Absolute temperature	K
V	volume of solution in reactor	L
x_f	film thickness surrounding adsorbent	m
y	distance from membrane	m

GREEK LETTERS

μ	viscosity of permeate	s^{-1}
ρ	density	$kg.m^{-3}$

REFERENCES

Adams, M.D., "**The Chemical Behaviour of Cyanide in the Extraction of Gold 1. Kinetics of Cyanide Loss in the Presence and Absence of Activated Carbon**", *J. S. Afr. Inst. Min. Metall.*, Vol. 90, No. 2, pp 37-44 (1990)

Adams, M.D., and Fleming, C.A., "**The Mechanism of Adsorption of Aurocyanide onto Activated Carbon**", *Metallurgical Transactions*, Vol. 20B, pp 315-325 (June 1989)

Adamson, R.J. (Editor), "**Gold Metallurgy in South Africa**", *Chamber of Mines of South Africa*, Chapter 1, 2, 4, 10, pp 1-55, 88-119, 284-347 (1972)

Bailey, P.R., "**The Extractive Metallurgy of Gold in South Africa**", The South African Institute of Mining and Metallurgy, (Editor: Stanley, G.G.), Vol. 1, Chapter 9, pp 379-449 (1987)

Balci, S., Dogu, T., and Yucel, H., "**Characterization of Activated Carbon Produced from Almond Shell and Hazelnut Shell**", *Journal Chem. Tech. Biotechnol.*, Vol. 60, pp 419-426 (1994)

Betty, R.L., "**Extruded Carbon; Gold Adsorption, Applications, and Attrition**", *Engineering and Mining Journal*, Vol. 195, pp 30-31 (June 1994)

Bhappu, R.B., "**Hydrometallurgical Processing of Precious Metal Ores**", *Mineral Processing and Extractive Metallurgy Review*, Vol. 6, pp 191-216 (1990)

Bokros, J.C., "**Chemistry and Physics of Carbon**", Marcel Dekker, New York, (Editor: P.C. Walker), 1969, pp 1-118

Coulson, J.M., and Richardson, J.F., "**Chemical Engineering**", Pergamon Press, (Editor: J.F., Richardson and D.G. Peacock), Vol. 3, pp 44-49

Dahya, A.S., and King, D.J., "**Developments in Carbon-in-Pulp technology for gold recovery**", CIM Bulletin, Vol. 76, pp 55-61, (Sept 1983)

Davidson, R.J., "**A Pilot Plant Study on the Effects of Cyanide Concentration of the CIP Process**", *Gold 100: Proceedings of the International Conference on Gold. Vol. 2: Extractive Metallurgy of Gold* (Editors: Fivax, C.E., and King, R.P.), The South African Institute of Mining and Metallurgy, Johannesburg, pp 209-223 (1986)

Davidson, R.J., "**The Mechanism of Gold Adsorption on Activated Charcoal**" *J. S. Afr. Inst. Min. Metall.*, Vol. 75, No. 4, pp 67-74 (Nov 1974)

Davidson, R.J., Douglas, W.D., and Tumilty, J.A., " **Aspects of Laboratory and Pilot Plant Evaluation of CIP with Relation to Gold Recovery**", *XIV International Minerals Processing Congress*, Canadian Institute of Mining and Metallurgy, Toronto, pp 6.1 - 6.19 (Oct 1982)

de Jong, I., "**Trace Cyanide Removal by Means of Silver Impregnated Active Carbon**", A Technical Report Written for the Technische Universiteit Delft, (June 1991)

Fast, J.L., "**Carbon-in-pulp pioneering at the Carlton Mill**", *Engineering and Mining Journal*, No. 56 (June 1988)

Fleming, C.A., Nicol, M.J., and Nicol, D.I., "**The optimisation of a carbon-in-pulp adsorption circuit based on the kinetics of extraction of aurocyanide by activated carbon**", Mintek confidential communication, No. C450.

Fleming, C.A., and Nicol, M.J., "**The Absorption of Gold Cyanide onto Activated Carbon: III Factors Influencing the Rate of Loading and the Equilibrium Capacity**", *J. S. Afr. Inst. Min. Metall.*, Vol. 84, No. 4, pp 85-93 (April 1984)

Gujarati, D.N., "**Basic Economics**", McGraw-Hill International Editions, 2nd Edition, Chapters 9-12 (1988)

Hall, K.B., "**Homestakes Uses Carbon-in-Pulp to Recover Gold from Slimes**", *World Mining*, Vol. 27, pp 44-49 (Nov 1974)

Hassler, J.W., "**Purification with Activated Carbon**", (3rd Edition), Published by Chemical Publishing Co. Inc., (New York), Chapter 11, pp 169-199 (1974)

Ibrado, A.S., and Fuerstenau, D.W., "**Effect of the Structure of Carbon Adsorbents on the Adsorption of Gold Cyanide**", *Hydrometallurgy*, Vol. 30, pp 243-256 (1992)

Jones, R.L., and Chandler, H.D., "**The effect of drag-reducing additives on the rheological properties of silica-water syspensions containing iron(III)oxide and of a typical gold-mine slurry**", *J. S. Afr. Inst. Min. Metall.*, Vol. 89, No. 6, pp 187-191 (June 1989)

La Brooy, S.R., Bax, A.R., Muir, D.M., Hosking, J.W., Hughes, H.C., and Parentich, A., "**Fouling of Activated Carbon by Circuit Organics**", *Gold 100: Proceedings of the International Conference on Gold. Vol. 2: Extractive Metallurgy of Gold* (Editors: Fivax, C.E., and King, R.P.), The South African Institute of Minign and Metallurgy, Johannesburg, pp 123-132 (1986)

La Brooy, S.R., Linge, H.G., and Walker, G.S., "**Review of Gold Extraction from Ores**", *Minerals Engineering*, Vol. 7, No. 10, pp 1213-1241 (1994)

Laxen, P.A., Becker, G.S.M., and Rubin, R., "**Development in the application of carbon-in-pulp to the recovery of gold from South African ores**", *J. S. Afr. Inst. Min. Metall.*, Vol. 79, No. 11, pp 315-326 (March 1994)

Laxen, P.A., Fleming, C.A., Holtum, D.A., and Rubin, R., "**A review of pilot-plant testwork conducted on the carbon-in-pulp process for the recovery of gold**", Proceedings, 12th CMMI Congress, The South African Institute of Mining and Metallurgy, (Editor - H.W. Glen), Vol 2, pp 551-561

Liebenberg, S.P., and van Deventer, J.S.J., "**The Realistic Simulation of CIP Plants Using Practical Measures of Competitive Adsorption and Fouling**", *Proceedings of the XX IMPC - Aachen*, pp 381-389 (Sept 1997)

Mattson, J.S., and Mark, H.B.(Jr), "**Activated Carbon: Surface Chemistry and Adsorption from Solution**", Published by Marcel Dekker, Inc., New York, Chapters 1-3, pp 1-37 (1971)

McBain, J.W., and Sessions, R.F., *Physical Chemistry*, Vol. 40, No. 603 (1936)

McDougall, G.J., "**The Physical Nature and Manufacture of Activated Carbon**", *Journal of the South African Institute of Mining and Metallurgy*, Vol. 91, No. 4, pp 109-120 (April 1991)

McDougall, G.J., and Hancock, R.D., "**Gold Complexes and Activated Carbon**", *Gold Bulletin*, Vol. 14, No. 4, pp 138-153 (1981)

McDougall, G.J., Hancock, R.D., Nicol, M.J., Wellington, O.L., and Copperthwaite, R.G., "**The Mechanism of the Adsorption of Gold Cyanide on Activated Carbon**", *J. S. Afr. Inst. Min. Metall.*, Vol 80, pp 344-356 (Sept 1980)

Menne, D., "**Optimization of Full-Scale Circuits for the Carbon-in-Pulp Recovery of Gold**", *Proceedings, 12th CMMI Congress*, The South African Institute of Mining and Metallurgy, Johannesburg, (Editor". Glen, H.W.), pp 569-574 (1982)

Menne, D., "**Predicting and Assessing Carbon-in-Pulp Circuit Performance**", *XIV International Minerals Processing Congress*, Canadian Institute of Mining and Metallurgy, Toronto, pp 5.1 - 5.19 (Oct 1982)

Minison, D.N., "**The Linear Screen: A Major Development in screening for the Gold Industry**", *Gold 100: Proceedings of the International Conference on Gold. Vol. 2: Extractive Metallurgy of Gold* (Editors: Fivax, C.E., and King, R.P.), The South African Institute of Minign and Metallurgy, Johannesburg, pp 97-110 (1986)

Petersen, F.W., and van Deventer, J.S.J., "**The influence of pH, Dissolved Oxygen and Organics on the Adsorption of Metal Cyanides on Activated Carbon**", *Chemical Engineering Science*, Vol. 46, No. 12, pp 3053-3065 (1991)

Petersen, F.W., van Deventer, J.S.J., an Lorenxen, L., "**The Ineraction Between Metal Cyanides, Fine Particles and Porous Adsorbents in an Agitated Slurry**", *Chemical Engineering Science*, Vol. 48, No. 16, pp 2919-2925 (1993)

Petruk, W., "**Recent progress in mineralogical investigations related to gold recovery**", CIM Bulletin, pp 37-39 (Nov 1989)

Schubert, J.H., Barker, I.J., and Swartz, C.L.E., "**Performance evaluation of a carbon-in-pulp plant by dynamic simulation**", *J. S. Afr. Inst. Min. Metall.*, Vol. 93, No. 11/12, pp 293-299 (Nov/Dec 1993)

Sorensen, P.F., "**The Origins and Treatment of Fine Carbon in Carbon-in-Pulp Plants**", *Mine Metallurgical Managers' Association, The Role of the Practical Metallurgist, Syposium*, pp 98-120 (June 1989)

Stange, W., "**The optimization of the CIP process using mathematical and economic models**", *Minerals Engineering*, Vol. 4, No. 12, pp 1279-1295 (1991)

Stange, W., Woollacott, L.C., and King, R.P., "**Towards more effective simulation of CIP and CIL process. 3. Validation and use of a new simulator**", *J. S. Afr. Inst. Min. Metall.*, Vol. 90, No. 12, pp 323-331 (Dec 1990)

Stanley, G.G., "**Gold Extraction Plant Practice in South Africa**", *Mineral Processing and Extractive Metallurgy Review*, Vol. 6, pp 191-216 (1990)

van Dam, H.E., "**Wet Attrition Tests for CIP/CIL carbons**" *Engineering and Mining Journal*, Vol 194, pp 44-45 (Feb 1993)

van Dam, H.E., "**Gold Recovery Carbons; Durability as a Consequence of Structure**", *Engineering and Mining Journal*, Vol. 196, pp 26-28 (April 1995)

van Deventer, J.S.J., "**Kinetic model for the adsorption of metal cyanides on activated charcoal**", Ph.D Thesis, University of Stellenbosch (1984)

van Deventer, J.S.J., "**Factors Influencing the Efficiency of a Carbon-in-Pulp Adsorption Circuit for the Recovery of Gold from Cyanided Pulp**", *Gold 100: Proceedings of the International Conference on Gold. Vol. 2: Extractive Metallurgy of Gold* (Editors: Fivax, C.E., and King, R.P.), The South African Institute of Minign and Metallurgy, Johannesburg, pp 85-95 (1986)

Wan, R.Y., and Miller, J.D., "**Research and Development Acrivities for the Recovery of Godl from Alkaline Cyanide Solutions**", *Mineral Processing and Extractive Metallurgy Review*, Vol. 6, pp 143-190 (1990)

Wang, X., and Forssberg, E.K.S., "**The Chemisty of Cyanide-Metal Complexes in Relation to Hydrometallurgical Processes of precious Metals**", *Mineral Processing and Extractive Metallurgy Review*, Vol. 6, pp 81-125 (1990)

Weber Jr, W.J., and Smith, E.H., "**Simulation and design models for adsorption processes**", *Environmental Science and Technology*, Vol. 21, No. 11, pp 1040-1050 (1987)

Woollacott, L.C., and Erasmus, C.S., "**The distribution of gold on loaded carbon**", *J. S. Afr. Inst. Min. Metall.*, Vol. 92, No. 7, pp 177-182 (July 1992)

Woollacott, L.C., and Nino de Guzman, G., "**The isotherm shift in carbon-in-pulp adsorption circuit**", *J. S. Afr. Inst. Min. Metall.*, Vol. 93, No. 8, pp 185-193 (Aug 1993)

Woollacott, L.C., Stange, W., and King, R.P., "**Towards more effective simulation of CIP and CIL process. 1. The modelling of adsorption and leaching**", *J. S. Afr. Inst. Min. Metall.*, Vol. 90, No. 10, pp 275-282 (Oct 1990)

Yannopoulos, J.C., "**The Extractive Metallurgy of Gold**", Published by Von Nostrand Reinhold (New York), Chapters 3-5, 8, 10-11, pp 25-114, 141-170, 185-256 (1990)

Young, G.J.C., Douglas, W.D., and Hampshire, M.J., "**Carbon in pulp process for recovering gold from acid plant calcines at Presedent Brand**" *Mining Engineering*, Vol. 36, No. 3, pp 257-264 (1984)

Zadra, J.B., Eagel, A.L., and Aeimen, H.J., "**Process for the recovery of gold and silver from activated carbon by leaching and electrolysis**:, US, Bureau of Mines, Report of investigations, No. 4843 (1952)

APPENDIX A

RAW DATA

FROM

STIRRING SPEED EXPERIMENTS

Stirring Speed Experiment

Conditions:

The various densities were made up using distilled water.

Slurry Density ($kg.m^{-3}$)	Minimum Stirring Speed (rpm)	Reynolds Number	Power Number
1050	385	0.00144	14545
1100	400	0.00163	15107
1150	410	0.00179	15480
1200	425	0.00203	15879
1300	460	0.00261	15884
1500	520	...	...
1600	700	...	...

APPENDIX B

RAW DATA

FROM

ISOTHERM EXPERIMENT

Isotherm Experiment

Conditions

Slurry density: Clear solution

Stirring speed: 300 rpm

Initial gold concentration: 0.5 $g.l^{-1}$

Running time: 72 hours

pH: 11

Time	**Initial Gold Concentrations**				
(Hours)	**5 ppm**	**10 ppm**	**15 ppm**	**20 ppm**	**30 ppm**
0	5.154	10.620	15.779	19.558	30.081
72	1.732	2.396	4.490	8.985	14.195

APPENDIX C

RAW DATA

FROM

BATCH EXPERIMENTS

Experiment 1, 2 and 3

Conditions

Slurry density: 1100kg.m^{-3}

Stirring speed: 400 rpm (Minimum stirring speed)

Initial gold concentration: 10 ppm

Running time: 5 hours

pH: 11

Time	**Mass of carbon**		
(Minutes)	**1 g**	**2 g**	**3 g**
0	10.33	10.22	10.30
10	9.16	8.46	6.39
20	8.27	6.86	4.27
30	7.60	5.68	3.11
60	5.65	3.30	1.20
120	3.53	1.34	0.30
180	1.97	0.56	0.04
240	1.41	0.31	0.04
300	0.91	0.15	0.00

Experiment 4, 5 and 6

Conditions

Slurry density: 1100kg.m^{-3}

Stirring speed: 400 rpm (Minimum stirring speed)

Initial gold concentration: 7 ppm

Running time: 5 hours

pH: 11

Time	**Mass of carbon**		
(Minutes)	**1 g**	**2 g**	**3 g**
0	7.20	6.97	7.07
10	6.72	5.42	4.11
20	6.24	4.18	2.95
30	5.72	3.35	1.94
60	4.11	1.80	0.73
120	2.81	0.51	0.09
180	1.81	0.20	0.04
240	1.24	0.05	0.00
300	0.81	0.05	0.00

Experiments 7, 8 and 9

Conditions

Slurry density: 1100 $kg.m^{-3}$

Stirring speed: 400 rpm (Minimum stirring speed)

Initial gold concentration: 5 ppm

Running time: 5 hours

pH: 11

Time	**Mass of carbon**		
(Minutes)	**1 g**	**2 g**	**3 g**
0	5.00	4.94	5.01
10	4.61	3.73	3.11
20	4.06	3.04	2.15
30	3.67	2.36	1.41
60	2.78	1.15	0.51
120	1.56	0.15	0.04
180	0.90	0.00	0.00
240	0.35	0.00	0.00
300	0.18	0.00	0.00

Experiments 10, 11 and 12

Conditions

Slurry density: 1100 $kg.m^{-3}$

Stirring speed: 460 rpm

Initial gold concentration: 10 ppm

Running time: 5 hours

pH: 11

Time	**Mass of carbon**		
(minutes)	**1 g**	**2 g**	**3 g**
0	10.44	9.86	9.88
10	9.46	7.43	6.09
20	8.48	5.83	4.00
30	7.86	4.64	2.58
60	6.21	2.42	0.88
120	4.15	0.77	0.16
180	2.86	0.25	0.11
240	1.93	0.20	0.11
300	1.36	0.10	0.11

Experiments 13, 14 and 15

Conditions

Slurry density: 1100 $kg.m^{-3}$

Stirring speed: 460 rpm

Initial gold concentration: 7 ppm

Running time: 5 hours

pH: 11

Time	**Mass of carbon**		
(Minutes)	**1 g**	**2 g**	**3 g**
0	7.62	7.18	7.10
10	6.71	5.43	4.75
20	6.13	4.24	3.43
30	5.54	3.26	2.61
60	4.21	1.67	1.24
120	2.56	0.48	0.42
180	1.60	0.18	0.22
240	0.97	0.12	0.01
300	0.65	0.07	0.01

Experiments 16, 17 and 18

Conditions

Slurry density: 1100 $kg.m^{-3}$

Stirring speed: 460 rpm

Initial concentration: 5 ppm

Running time: 5 hours

pH: 11

Time	**Mass of carbon**		
(Minutes)	**1 g**	**2 g**	**3 g**
0	5.29	4.58	5.15
10	4.98	3.34	3.08
20	4.50	2.43	2.10
30	4.16	1.89	1.48
60	3.20	0.71	0.55
120	2.07	0.28	0.24
180	1.37	0.17	0.19
240	0.94	0.12	0.03
300	0.63	0.12	0.03

Experiments 19, 20 and 21

Conditions

Slurry density: 1100 $kg.m^{-3}$

Stirring speed: 520 rpm

Initial concentration: 10 ppm

Running time: 5 hours

pH: 11

Time	**Mass of carbon**		
(Minutes)	**1 g**	**2 g**	**3 g**
0	10.09	10.26	9.93
10	9.17	7.64	5.82
20	8.41	6.15	3.73
30	7.64	4.97	2.41
60	5.79	2.56	0.71
120	3.55	0.77	0.27
180	1.81	0.15	0.00
240	1.54	0.00	0.00
300	1.10	0.00	0.00

Experiments 22, 23 and 24

Conditions

Slurry density: 1100 $kg.m^{-3}$

Stirring speed: 520 rpm

Intial gold concentration: 7 ppm

Running time: 5 hours

pH: 11

Time	**Mass of carbon**		
(Minutes)	**1 g**	**2 g**	**3 g**
0	7.59	6.36	7.05
10	7.05	4.48	3.78
20	6.33	3.42	2.31
30	5.91	2.66	1.44
60	4.71	1.19	0.47
120	3.21	0.32	0.17
180	2.18	0.17	0.01
240	1.58	0.17	0.01
300	1.10	0.17	0.01

Experiments 25, 26 and 27

Conditions

Slurry density: 1100 $kg.m^{-3}$

Stirring speed: 520 rpm

Initial gold concentration: 5 ppm

Running time: 5 hours

pH: 11

Time	**Mass of carbon**		
(Minutes)	**1 g**	**2 g**	**3 g**
0	5.31	5.38	4.96
10	4.77	3.63	2.87
20	4.47	2.84	1.80
30	4.05	2.26	1.19
60	3.21	1.20	0.42
120	1.94	0.30	0.12
180	1.28	0.04	0.00
240	0.92	0.00	0.00
300	0.68	0.00	0.00

Experiments 28, 29 and 30

Conditions

Slurry density: 1300 $kg.m^{-3}$

Stirring speed: 450 rpm

Initial gold concentration: 10 ppm

Running time: 5 hours

pH: 11

Time	**Mass of carbon**		
(Minutes)	**1 g**	**2 g**	**3 g**
0	10.21	9.99	9.36
10	9.03	7.99	5.54
20	7.80	6.25	3.45
30	7.11	5.04	2.38
60	5.19	2.89	0.77
120	2.95	1.04	0.50
180	1.72	0.36	0.28
240	1.13	0.10	0.00
300	0.71	0.04	0.00

Experiments 31, 32 and 33

Conditions

Slurry density: 1300 $kg.m^{-3}$

Stirring speed: 450 rpm

Intial gold concentration: 7 ppm

Running time: 5 hours

pH: 11

Time	**Mass of carbon**		
(Minutes)	**1 g**	**2 g**	**3 g**
0	7.14	7.15	6.56
10	6.37	4.60	3.72
20	5.72	3.63	2.48
30	5.06	2.84	1.73
60	3.69	1.65	0.44
120	2.16	0.74	0.12
180	1.22	0.51	0.12
240	0.79	0.34	0.12
300	0.51	0.23	0.12

Experiments 34, 35 and 36

Conditions

Slurry density: 1300 $kg.m^{-3}$

Stirring speed: 450 rpm

Intial gold concentration: 5 ppm

Running time: 5 hours

pH: 11

Time	**Mass of carbon**		
(Minutes)	**1 g**	**2 g**	**3 g**
0	5.05	5.21	4.52
10	4.23	4.18	2.48
20	3.90	3.15	1.62
30	3.57	2.53	0.99
60	2.53	1.23	0.23
120	1.71	0.41	0.00
180	0.83	0.10	0.00
240	0.28	0.00	0.00
300	0.12	0.00	0.00

Experiments 37, 38 and 39

Conditions

Slurry density: 1300 $kg.m^{-3}$

Stirring speed: 520 rpm

Intial gold concentration: 10 ppm

Running time: 5 hours

pH: 11

Time	**Mass of carbon**		
(Minutes)	**1 g**	**2 g**	**3 g**
0	10.59	10.22	9.52
10	9.53	6.70	5.44
20	8.68	5.34	3.61
30	8.15	4.26	2.43
60	6.34	2.61	0.77
120	3.84	1.19	0.28
180	2.35	0.68	0.00
240	1.55	0.45	0.00
300	0.97	0.28	0.00

Experiments 40, 41 and 42

Conditions

Slurry density: 1300 $kg.m^{-3}$

Stirring speed: 520 rpm

Intial gold concentration: 7 ppm

Running time: 5 hours

pH: 11

Time	**Mass of carbon**		
(Minutes)	**1 g**	**2 g**	**3 g**
0	7.21	7.08	6.75
10	6.88	5.58	3.73
20	6.12	4.80	2.52
30	5.52	1.42	1.70
60	4.26	0.49	0.55
120	2.74	0.25	0.16
180	1.70	0.25	0.00
240	1.10	0.25	0.00
300	0.88	0.25	0.00

Experiments 43, 44 and 45

Conditions

Slurry density: 1300 $kg.m^{-3}$

Stirring speed: 520 rpm

Intial gold concentration: 5 ppm

Running time: 5 hours

pH: 11

Time	**Mass of carbon**		
(Miutes)	**1 g**	**2 g**	**3 g**
0	5.33	5.06	4.94
10	4.79	2.79	2.47
20	4.31	2.22	1.54
30	3.94	1.80	0.93
60	2.92	1.08	0.27
120	1.85	0.46	0.00
180	1.11	0.25	0.00
240	0.68	0.10	0.00
300	0.52	0.15	0.00

Experiments 46, 47 and 48

Conditions

Slurry density: 1300 $kg.m^{-3}$

Stirring speed: 590 rpm

Intial gold concentration: 10 ppm

Running time: 5 hours

pH: 11

Time	**Mass of carbon**		
(Minutes)	**1 g**	**2 g**	**3 g**
0	9.94	10.27	10.09
10	8.91	7.38	4.80
20	7.83	5.38	3.16
30	6.99	4.09	2.00
60	4.87	1.98	0.67
120	2.90	0.59	0.09
180	1.68	0.28	0.04
240	1.02	0.18	0.04
300	0.69	0.12	0.00

Experiments 49, 50 and 51

Conditions

Slurry density: 1300 $kg.m^{-3}$

Stirring speed: 590 rpm

Intial gold concentration: 7 *ppm*

Running time: 5 hours

pH: 11

Time	**Mass of carbon**		
(Minutes)	**1 g**	**2 g**	**3 g**
0	6.80	7.08	7.08
10	6.09	4.92	2.85
20	5.39	3.85	1.64
30	4.92	3.13	0.27
60	3.89	0.87	0.11
120	2.34	0.15	0.00
180	1.49	0.00	0.00
240	0.97	0.00	0.00
300	0.79	0.00	0.00

Experiments 52, 53 and 54

Conditions

Slurry density: 1300 $kg.m^{-3}$

Stirring speed: 590 rpm

Initial gold concentration: 5 ppm

Running time: 5 hours

pH: 11

Time	**Mass of carbon**		
(Minutes)	**1 g**	**2 g**	**3 g**
0	5.30	5.27	4.94
10	4.59	3.42	2.47
20	4.21	2.60	1.48
30	3.83	1.93	0.99
60	2.95	0.90	0.27
120	1.81	0.23	0.00
180	1.21	0.07	0.00
240	0.88	0.07	0.00
300	0.72	0.02	0.00

Experiments 55, 56 and 57

Conditions

Slurry density: 1500 $kg.m^{-3}$

Stirring speed: 520 rpm

Initial gold concentration: 10 ppm

Running time: 5 hours

pH: 11

Time	**Mass of carbon**		
(Minutes)	**1 g**	**2 g**	**3 g**
0	10.19	10.05	10.00
10	8.50	5.06	7.22
20	8.17	3.99	5.94
30	7.57	3.22	4.82
60	5.98	1.90	2.65
120	4.66	0.83	0.98
180	3.35	0.47	0.37
240	2.64	0.37	0.15
300	1.98	0.32	0.09

Experiments 58, 59 and 60

Conditions

Slurry density: 1500 $kg.m^{-3}$

Stirring speed: 520 rpm

Initial gold concentration: 7 ppm

Running time: 5 hours

pH: 11

Time	**Mass of carbon**		
(Minutes)	**1 g**	**2 g**	**3 g**
0	6.80	7.10	6.68
10	5.43	3.89	3.97
20	4.99	3.33	3.04
30	4.61	2.97	2.42
60	3.68	2.15	1.58
120	2.26	1.13	0.49
180	1.43	0.73	0.29
240	1.11	0.52	0.08
300	0.56	0.42	0.00

Experiments 61, 62 and 63

Conditions

Slurry density: 1500 $kg.m^{-3}$

Stirring speed: 520 rpm

Initial gold concentration: 5 ppm

Running time: 5 hours

pH: 11

Time	**Mass of carbon**		
(Minutes)	**1 g**	**2 g**	**3 g**
0	5.11	5.16	5.11
10	4.57	2.43	1.90
20	3.96	1.80	1.48
30	3.74	1.38	1.17
60	3.03	0.75	0.69
120	1.99	0.27	0.33
180	1.22	0.12	0.27
240	0.84	0.06	0.12
300	0.57	0.00	0.12

Experiments 64, 65 and 66

Conditions

Slurry density: 1500 $kg.m^{-3}$

Stirring speed: 600 rpm

Initial gold concentration: 10 *ppm*

Running time: 5 hours

pH: 11

Time	**Mass of carbon**		
(Minutes)	**1 g**	**2 g**	**3 g**
0	10.09	9.64	9.83
10	5.94	5.12	5.35
20	5.03	4.13	4.00
30	4.28	3.20	2.87
60	2.93	1.84	1.36
120	1.64	0.81	0.44
180	0.94	0.39	0.28
240	0.62	0.23	0.17
300	0.46	0.23	0.11

Experiments 67, 68 and 69

Conditions

Slurry density: 1500 $kg.m^{-3}$

Stirring speed: 600 rpm

Initial gold concentration: 7 ppm

Running time: 5 hours

pH: 11

Time	Mass of carbon		
(Minutes)	1 g	2 g	3 g
0	7.29	6.07	6.03
10	4.11	3.78	2.83
20	3.68	3.15	2.08
30	3.36	2.68	1.65
60	2.71	1.93	1.14
120	1.85	1.22	0.82
180	1.37	0.94	0.74
240	0.83	0.86	0.70
300	0.72	0.78	0.70

Experiments 70, 71 and 72

Conditions

Slurry density: 1500 $kg.m^{-3}$

Stirring speed: 600 rpm

Initial gold concentration: 5 ppm

Running time: 5 hours

pH: 11

Time	Mass of carbon		
(Minutes)	1 g	2 g	3 g
0	4.53	5.08	5.08
10	3.15	3.03	2.22
20	2.91	2.33	1.57
30	2.56	1.95	1.14
60	2.08	1.14	0.55
120	1.49	0.55	0.28
180	1.33	0.33	0.17
240	1.06	0.17	0.17
300	0.98	0.17	0.11

Experiments 73, 74 and 75

Conditions

Slurry density: 1500 $kg.m^{-3}$

Stirring speed: 680 rpm

Initial gold concentration: 10 ppm

Running time: 5 hours

pH: 11

Time	**Mass of carbon**		
(Minutes)	**1 g**	**2 g**	**3 g**
0	9.94	9.99	9.65
10	7.66	5.79	4.77
20	6.10	4.49	3.41
30	5.21	3.52	2.55
60	3.88	2.04	1.25
120	2.71	0.96	0.45
180	1.98	0.57	0.28
240	1.54	0.40	0.17
300	1.20	0.28	0.11

Experiments 76, 77 and 78

Conditions

Slurry density: 1500 $kg.m^{-3}$

Stirring speed: 680 rpm

Initial gold concentration: 7 ppm

Running time: 5 hours

pH: 11

Time	**Mass of carbon**		
(Minutes)	**1 g**	**2 g**	**3 g**
0	6.47	6.39	6.49
10	3.35	3.34	2.41
20	2.99	2.46	1.58
30	2.68	2.10	1.17
60	2.05	1.07	0.40
120	1.17	0.24	0.03
180	0.75	0.03	0.00
240	0.44	0.00	0.00
300	0.29	0.00	0.00

Experiments 76, 77 and 78

Conditions

Slurry density: 1500 $kg.m^{-3}$

Stirring speed: 680 rpm

Initial gold concentration: 7 ppm

Running time: 5 hours

pH: 11

Time	**Mass of carbon**		
(Minutes)	**1 g**	**2 g**	**3 g**
0	6.47	6.39	6.49
10	3.35	3.34	2.41
20	2.99	2.46	1.58
30	2.68	2.10	1.17
60	2.05	1.07	0.40
120	1.17	0.24	0.03
180	0.75	0.03	0.00
240	0.44	0.00	0.00
300	0.29	0.00	0.00

Experiments 79, 80 and 81

Conditions

Slurry density: 1500 $kg.m^{-3}$

Stirring speed: 680 rpm

Initial gold concentration: 5 ppm

Running time: 5 hours

pH: 11

Time	**Mass of carbon**		
(Minutes)	**1 g**	**2 g**	**3 g**
0	5.05	5.05	5.05
10	3.83	2.60	2.20
20	3.01	2.13	1.72
30	2.47	1.79	1.18
60	1.99	1.18	0.63
120	1.24	0.63	0.34
180	0.90	0.50	0.29
240	0.77	0.43	0.29
300	0.70	0.36	0.29